Interaction with phospho-eIF4E commits S6 Kinase 1 for mTORC2 and PHLPP1 mediated activation.

Sheikh Tahir Majeed[1]; Asiya Batool[1]; Rabiya Majeed[1, 2]; Nadiem Nazir Bhat[1]; Khurshid Iqbal Andrabi[1*]

[1] Department of Biotechnology, University of Kashmir, J&K- India.
[2] Department of Biochemistry, University of Kashmir, J&K- India.
***Address for correspondence andrabik@uok.edu.in**

Abstract

Eukaryotic initiation factor (eIF4E) phosphorylation is a recognized attribute for enhanced cell growth and proliferation. Our recent data that identified eIF4E as mTORC1 substrate with ability to influence rapamycin response highlights its prospect as a mediator of mTORC1 signaling. Here, we present evidence that eIF4E phosphorylated at S209 interacts with TOS motif of S6 Kinase1 (S6K1). We show that this interaction is sufficient to overcome rapamycin sensitivity and mTORC1 dependence of S6K1. We present data to demonstrate that eIF4E-S6K1 interaction relieves S6K1 of its auto inhibition, otherwise rate limiting for its activation. We go on to identify a highly conserved sequence segment that mediates hydrophobic motif phosphorylation of S6K1 in mTORC2 rather than mTORC1 dependent manner. We also identify a novel eight amino-acid PHLPP1 (Pleckstrin Homology Domain Leucine-rich Repeat Protein Phosphatase) binding region necessary to mediate S6K1 response to serum/growth factor stimulation. Finally, we show that deletion of the PHLPP1 binding region abolishes serum/growth factor stimulatory response without interfering with S6K1 regulation by mTORC1 or mTORC2. Our data identifies eIF4E as a novel TOS binding subunit that realigns mTORC1 signaling to unravel cross talk with other growth promoting signals for accomplishing S6K1 activation.

Key Words: mTOR, S6 Kinase 1, eIF4E, PHLPP1, Rapamycin,

Introduction

Mechanistic target of rapamycin complex 1 (mTORC1) holds the centre stage for regulating cell growth and proliferation. mTORC1 gets activated by sensing nutrient, growth factor signals and mediates a stimulatory effect on key cellular functions like cap-dependent translation and cell cycle progression (Saxton and Sabatini, 2017). This growth regulating attribute of mTORC1 is accomplished through two of its major substrates, S6 Kinase 1(S6K1)) (Majeed, S.T.; Majeed, R.; Shah, G.; Andrabi, 2019), a member of AGC family of protein kinases (Powers, 2007) and 4EBP1(Schalm et al., 2003) . Both these substrates are shown to use special sequence motif, TOS (TOR signaling) to interact with activated mTORC1 through its adaptor protein, raptor(Nojima et al., 2003; Schalm et al., 2003). This interaction is believed to result in phosphorylation of S6K1at Thr412 position which is present in its hydrophobic motif (HM) and is an exception to other AGC kinases which mainly rely on mTORC2 rather than mTORC1 for this event (García-

Martínez and Alessi, 2008). While the loss of HM phosphorylation, either due to inhibition by rapamycin or impeded recruitment of raptor due to TOS mutation/disruption, endorses the dependence of HM phosphorylation on the activation state of mTORC1, identification of HM phosphorylation in S6K1 mutants with TOS dysfunction and C-terminal auto inhibitory domain deletion(Ali and Sabatini, 2005; Dennis et al., 2001), suggests that inhibition due to rapamycin may be mediated by an event distinct from the one that influences HM phosphorylation. This is consistent with our own data that highlights disconnect between HM phosphorylation and rapamycin response by S6K1 to foster the argument that loss of phosphorylation may be a consequence rather than a mechanistic basis of mTORC1 inhibition (Beigh et al., 2012; Beigh et al., 2013). While identification of new mTORC1 substrates, without a consensus TOS motif (Hong et al., 2017; Kim et al., 2011; Koren et al., 2010) undermines the centrality of TOS in mediating raptor binding, data highlighting the ability of raptor-free mTORC1 to phosphorylate S6K1(Yip et al., 2010) and the inconsistent stature of mTORC1 as a 4EBP1 kinase *in vivo* (Ito et al., 2016), adds further credence to the narrative. Our recent observation that identifies eIF4E rather than raptor as the cellular factor regulating rapamycin response further deepens the disconnect between mTORC1 regulation and S6K1 phosphorylation to uphold eIF4E as an emerging link in regulating rapamycin response (Batool, A.; Majeed, S.T.; Aashaq, S.; Majeed, R.; Shah, G.; Nazir, N.; Andrabi, 2019). We have also identified eIF4E as a novel member of the mTORC1 pathway whose phosphorylation by mTORC1, and feedback phosphorylation by map kinase interacting kinase (MNK) kinase, puts forth a fresh perspective of signaling downstream of mTORC1, especially in the context of its possible interaction with S6K1(Batool et al., 2020). We therefore assessed whether eIF4E influences the state of S6K1 regulation.

In this current study, we show that phosphorylated eIF4E, instead of raptor, interacts with S6K1-TOS motif. While this interaction imparts rapamycin resistance to S6K1, it further relieves inhibition by -NH2 and -COOH terminal domains and primes S6K1 for hydrophobic motif phosphorylation by mTORC2. We further identify eight amino-acid PHLPP1 binding region in S6K1 that is crucial for mediating serum response and as such is instrumental for complete activation of S6K1. Thus, we propose a mechanism for S6K1 activation wherein TOS serves to recruit eIF4E instead of raptor to propagate mTORC1 dependent priming that influences mTORC2 mediated S6K1 phosphorylation as a consequence.

Results

eIF4E phosphorylation governs S6K1 activation state.

Consistent with the tumorigenic attributes of eIF4E and S6K1 (Ben-Hur et al., 2013; Li et al., 2012; Martín et al., 2000; Siddiqui and Sonenberg, 2015; Zhang et al., 2019), we observed enhanced expression of both these proteins across various cancer cell lines compared to non-transformed HEK293 and NIH3T3 cells (Fig 1A). Furthermore, eIF4E and S6K1 exhibited increased expression pattern in primary human tumour samples, namely breast, gastric and colorectal (Fig1B). The overexpression of eIF4E and S6K1

corresponded with a concomitant increase in phosphorylation at Ser 209 and Thr 412 respectively, both in cancer tissues and cell lines (Fig 1C, D). To ensure that increase in the phosphorylation levels is not due to increased total protein levels in cancer samples, we optimized the total protein load such as to bring eIF4E and S6K1 protein levels in cancer samples at par with their corresponding control samples. However, this optimization deranged the pattern of loading control (Fig 1C, D). Based on these observations and some earlier studies that have aimed to establish a relationship between eIF4E stoichiometry and mTORC1 response (Alain et al., 2012; Josse et al., 2016), we explored whether eIF4E abundance/phosphorylation relates with the activation status of mTORC1. Accordingly, we transfected myc tagged eIF4E in HEK293 and NIH3T3 cells to assess the impact on the state of S6K1 activity which is normally used as a functional readout for mTORC1 activation (Yang et al., 2017). Ectopic expression of myc-eIF4E increased phosphorylation levels of S6K1 at Thr412 site and also furthered its ability to phosphorylate GST-S6 in an *in vitro* kinase assay (Fig IE). Alternatively, we achieved eIF4E stoichiometric abundance by shRNA mediated downregulation of its binding partner, 4EBP1 and expectedly observed an increase in S6K1 activation that was reversed by 4EBP1 replenishment (Fig 1F). Interestingly, the ability of rapamycin to inhibit S6K1 was overcome significantly during eIF4E overexpression (See supplementary Fig. S1). Together, these observations support a possible link between eIF4E stoichiometry/phosphorylation and mTORC1 response, and also concur with our recent finding that identifies eIF4E, and not raptor, as the cellular factor responsible for mediating rapamycin response(Batool, A.; Majeed, S.T.; Aashaq, S.; Majeed, R.; Shah, G.; Nazir, N.; Andrabi, 2019).

Since eIF4E abundance and phosphorylation exhibit strict dependence (Wendel et al., 2007), we examined whether the observed effect on S6K1 activation was governed by eIF4E phosphorylation. Lines of HEK293 cells stably expressing Flag tagged S6K1 were therefore established and transfected with myc tagged eIF4E or its Phosphodeficient (Ser209A) or Phospho mimicked (Ser209E) variants. As seen in fig 1G, the activity state of S6K1 was significantly enhanced upon transfection with eIf4E. Strikingly, the effect was further pronounced upon over expression of phosphomimicked eIf4E with near complete resistance to rapamycin. On the contrary, phosphodeficient eIF4E (Ser209A) was unable to influence S6K1 activity to any significant extent. These observations, though surprising, highlight a possible role for eIF4E phosphorylation in mediating mTORC1 response onto S6K1.

mTORC1 interacts with and phosphorylates eIF4E.

Having confirmed the role of eIF4E phosphorylation in mediating mTORC1 response on S6K1, we next chose to evaluate whether eIF4E phosphorylation was in any way responsive to the dynamics of mTORC1 activation. Since mTORC1 is sensitive to amino acids, glycolytic inhibitor-2deoxy glucose (2-DG) and rapamycin(Dennis et al., 2001), we used these inputs to assess their influence on eIF4E phosphorylation. Addition of rapamycin, 2-DG to HEK293 cells or amino-acid withdrawal caused significant reduction in

eIF4E phosphorylation (Fig 2A). The observed dependence of eIF4E phosphorylation on mTORC1 conformed with the ability of GST-4E to act as mTORC1 substrate *in vitro*, with faithful adherence to rapamycin inhibition (described by us previously (Batool et al., 2020), see also Supplementary Fig S2). To test this observation further, we generated cells wherein mTORC1 influence was mitigated using shRNA knockdown of mTOR kinase or its adaptor protein raptor and observed complete loss of 4E phosphorylation in both cases (Fig 2B). These results advocate that eIF4E phosphorylation was indeed dependent on mTORC1 response.

Since mTORC1 interacts with its substrates through raptor (Yang et al., 2017), we immunoprecipitated raptor from HEK293 cells co-transfected with HA-raptor and myc-eIF4E and found eIF4E was present in raptor immunoprecipitates (Fig 2C). Conversely, immunoprecipitates of ectopically expressed eIF4E also co- precipitated endogenous raptor (Fig 2D). We have previously identified TPTPNPP motif in eIf4E as a potential binding site for raptor(Batool et al., 2020). Since this sequence appeared to be conserved among several mTORC1 substrates (Fig 2D), we conducted flexible peptide propensity modelling of these sequence motifs (Kurcinski et al., 2015) and evaluated their binding potential with raptor. A probability index of more than 80% for all the sequences checked, suggested their relevance as signature motif for raptor binding. (Fig 2E; See also supplementary Fig. S3). We further, deleted this sequence from eIF4E, PRAS40 and ULK1 to assess the impact on raptor association. The immunoprecipitates of wild type eIF4E, PRAS40, ULK1 and their mutant forms, obtained from transfected HEK293T cells showed that the mutants failed to display any detectable co-precipitation of endogenous raptor as compared to their WT counterparts (Fig 2F). Together these results relate the said motif in mediating raptor binding and further highlight eIf4E as mTORC1 effector.

MNK1 mediated eIF4E Phosphorylation is a rapamycin activated feedback response.

Based on previous reports that identify MAP kinase interacting kinase 1 (MNK1) as eIF4E kinase (Proud, 2015; Shveygert et al., 2010) and the data reported herein, supporting mTORC1 dependence of eIF4E phosphorylation, we explored the involvement of MNK1 in eIF4E regulation. While the results in Fig 1A show high levels of eIF4E phosphorylation across various cancer cell lines, we asked whether MNK1 immunoprecipitated from these cell lines would cause more eIF4E phosphorylation as compared to HEK293 and NIH3T3 cell lines in an *in vitro* kinase assay. Surprisingly, MNK1 immunoprecipitates from these cell lines exhibited almost identical extent of GST-4E phosphorylation (Fig 3A). Additionally, MNK1 immunoprecipitates from Hela also produced similar results (Fig 3A). Furthermore, MNK1 immunoprecipitates from NIH3T3 and MCF7 cell lines, treated with different concentrations of MNK1 inhibitor, CGP57380, significantly reduced eIf4E phosphorylation at similar concentrations (Fig 3B). Together, these data rule out the activation of MNK1 as the basis for pronounced eIf4E phosphorylation *in*

vivo. Additionally, we tested the effect of rapamycin and MNK1 inhibitor in A549 and MCF7 cell lines. A 30 minute treatment with 50 nM rapamycin reduces the eIF4E phosphorylation while no such effect is observed after treatment with 10µM CGP57380 which is otherwise sufficient to inhibit MNK1 activity (Fig 3C). This was in tune with our recent data suggesting that MNK1 may not be the primary eIF4E kinase at least *in vivo* (Batool et al., 2020). To substantiate this observation further, we downregulated MNK1 expression using MNK1shRNA and observed that the phosphorylation state of eIF4E does not depend on MNK1 expression (Fig 3D). The results further advocate for a kinase other than MNK1 as a primary eIF4E kinase.

In the backdrop of data associating rapamycin with MNK activation(Brown and Gromeier, 2017; Stead and Proud, 2013), we have already shown that exposure of cells to rapamycin at concentrations (50nM) sufficient to inhibit mTORC1, correspond with inhibition of eIF4E phosphorylation that recovers over a period of 9-12 hours post rapamycin treatment due to feedback activation of MNK1 kinase(Batool et al., 2020) (see also supplementary information Fig. S 4 a,b). Interestingly, the phosphorylation recovers earlier when rapamycin is used at concentrations higher than 50nM (Fig 3E). In either case, the recovered phosphorylation remains sensitive to MNK inhibitor and is not registered in a MNK1 knockdown state (Fig 3F). Together these data demonstrate that MNK1 is indeed a feedback kinase for eIF4E.

eIF4E interacts with TOS motif of S6K1.

Having confirmed the dependence of eIF4E phosphorylation on mTORC1 activation and the role of MNK1 as feedback kinase for eIF4E, we further investigated how eIF4E phosphorylation regulates S6K1 activity. We have recently shown that phosphorylation of eIF4E at Ser209 site governs its binding with amino terminal region of S6K1(Batool et al., 2020). Here we examined if S6K1 activation, governed by the phosphorylation at Thr412 site, extends any influence on its interaction with eIF4E. Accordingly, HA tagged S6K1 alongside its phospho mutants, i.e. T412A and T412E, were co-transfected with myc-eIF4E in HEK293 cells and probed for any change in interaction. Both the mutant forms of S6K1 interacted with eIF4E with the same magnitude (Fig 4A). The results confirmed that the activating phosphorylation in S6K1 had no influence on its interaction with eIF4E. Since amino terminal region of S6K1 harbors TOS motif (Schalm and Blenis, 2002), we set out to investigate the relevance of this motif, if any, in mediating interaction with eIF4E. Accordingly, point mutants within and outside the TOS motif were constructed and evaluated for their influence on eIF4E interaction. While the mutations outside the TOS motif (F16A) did not hamper the interaction with eIF4E, mutation within the TOS motif (F28A) rendered S6K1 unable to bind eIF4E (Fig 4B). In addition, we used TOS motif sequences of S6K1 (FDIDL) and 4EBP1 (FEMDI) for *in silico* peptide propensity modelling to predict the prospect of TOS-eIF4E interaction. Fig 4C reveals that

eIF4E appeared to predict possible pocket for TOS binding with an RMSD value of 2.58 for FDIDL sequence and 1.6 for FEMDI sequence suggestive of a high possibility of TOS-eIF4E interaction (see also supplementary fig S5). We next used intact or disrupted TOS motif bearing peptides (FDIDL, ADIDL) in *in vitro* competition assays to assess whether either could compete out eIF4E-S6K1 interaction. Molar excess and above of intact TOS motif bearing peptide competed out S6K1 interaction with eIF4E (Fig 4D). Together, these data highlight the requirement of TOS motif for interaction with eIF4E.

While the prevailing view implicates TOS motif in raptor binding (Nojima et al., 2003), our recent data describes eIF4E as a raptor binding protein, instead (Batool et al., 2020). Hence, we set out to investigate if raptor could be an intermediate in eIF4E-TOS/S6K1 interaction. Raptor shRNA infected HEK293 cell lines were generated and transfected with myc-eIF4E and its phospho mutants (Ser209A, Ser209E), and examined for their ability to bind endogenous S6K1. While raptor knock down abrogates the interaction of WTeIF4E and its Phospho deficient variant (Ser209A) with S6K1, it could not abolish the interaction of S6K1 with phospho mimicked variant (Ser209E) of eIF4E (Fig 4E). These results suggest that raptor, though important for eIF4E phosphorylation, did not mediate eIF4E-S6K1 interaction. To validate this observation further, we used eIF4E truncation mutant (30-217), lacking raptor binding region (Batool et al., 2020), along with its phospho deficient, 30- 217(S209A), and phospho-mimicked, 30-217(S209E), variants to assess their ability to interact with S6K1 in comparison to WTeIF4E. While 30-217 and 30-217(S209A) variants of eIF4E failed to exhibit any detectable interaction with S6K1, phospho-mimicked form, 30-217(S209E) recovered its binding with S6K1 to near WT levels. Together, these data demonstrate that eIF4E-S6K1 interaction is solely governed by eIF4E phosphorylation at Ser209 site and is not mediated by raptor.

eIF4E- TOS interaction primes S6K1 for mTORC2 mediated activation.

TOS interaction with eIF4E, demonstrated herein, deviates from conventional understanding that implicates this motif with raptor/mTORC1 recruitment for direct phosphorylation and activation of S6K1(Nojima et al., 2003).The prevalent notion owes its origin to the failure of TOS mutant (F28A) or TOS-domain truncation variant (ΔNH) of S6K1 to display activating phosphorylation at its HM (Ali and Sabatini, 2005). We therefore, introduced a phosphomimicking mutation (T412E) in amino-terminus deletion variant of S6K1 to observe if the mutation would compensate for TOS dysfunction. Fig. 5A demonstrates that the mutant was unable to regain any detectable activity to indicate the redundancy of TOS for the occurrence of this phosphorylation. However, in agreement with published data (Ali and Sabatini, 2005), we observed complete recovery of HM phosphorylation upon truncating carboxy terminal domain (CTD) from S6K1 variant bearing TOS mutation (Fig 5B). Interestingly, the variant shows restoration of its serum response albeit to a lesser extent and remains rapamycin resistant (Fig 5B). The data suggests that TOS motif may be involved in the relief of inhibition caused by carboxy terminal domain. Interestingly, the double

truncation(Weng et al., 1995) (ΔNHΔCT) that rendered the enzyme active, fully phosphorylated at T412, exhibited complete recalcitrance to inputs known to inhibit mTORC1 (Fig.5C). This observation suggests that TOS-eIF4E interaction must relieve S6K1 of negative regulation to allow the HM phosphorylation and subsequent activation of the enzyme. Strikingly, selective sensitivity of this double truncation variant of S6K1 to Torin implicated mTORC2 rather than mTORC1 as the potential kinase to mediate HM phosphorylation (Fig 5D). We therefore went on to examine the state of S6K1 activation in the backdrop of mTORC2 compromise achieved in Rictor knock down cells. Accordingly, WTS6K1 or its double truncation mutant (ΔNHΔCT) was transfected in Rictor shRNA infected cells to detect any alterations in the magnitude of phosphorylation at T412. Phosphorylation in double truncation variant was dramatically reduced in Rictor knockdown cells as compared to the state of its phosphorylation in normal cells (Fig 5E). The magnitude of T412 loss in WTS6K1, although not so remarkable, appeared in tune with our contention that negative regulation due to TOS-CTD interplay undermines T412 phosphorylation in absence of growth factors. We therefore, chose to examine the knockdown effect of Rictor on serum response by S6K1. As seen in Fig.5F, serum stimulation of T412 phosphorylation was dramatically reduced in Rictor knockdown state hence demonstrating that this phosphorylation was indeed mediated by mTORC2 subject to disinhibition or priming by mTORC1.

A 19 amino-acid stretch of S6K1 mediates mTORC2 phosphorylation.

A careful examination of the sequence spanning the doubly truncated variant of S6K1 highlighted two important aspects. A consensus TOS motif in the middle of the catalytic domain (Fig.6A) and a highly conserved random loop sequence connecting amino terminal region with the catalytic domain (Fig.6B). Accordingly, we resorted to truncation mutagenesis to generate a variant of ΔNHΔCT, 147-421, bearing 100 amino acids deletion at its amino terminal end. This variant proximated the potential TOS motif at position 7 and as such represents a smaller version of S6K1. The aim was to examine whether the smaller size of the variant would better facilitate its random phosphorylation or indeed the presence of TOS would enhance its prospect of phosphorylation by mTORC1. However, the variant failed to display any detectable phosphorylation at T412, to clearly dispel the notion of the event being random, coincidental or non- physiological and implicate the truncated portion 47-146 in regulating HM phosphorylation (Fig 6C). Accordingly, we generated a series of smaller deletions across this 100 amino acid stretch to identify the sequence imparting regulation. Fig 6D shows that while HM phosphorylation was reasonably displayed in 77-421 and 91-421 variants, no such display was observed in 110-421 variant to narrow down the regulatory function within a 19 amino acid segment (91-109). Attempt to examine smaller deletions, 91- 99 and 100-109, within this

pleated stretch failed to reveal any further information due to the unreliable expression of these mutants. We therefore, chose to introduce this 19 amino acid deletion in a backdrop of WTS6K1 to address whether the presence of TOS bearing amino terminus and CTD would help the mutant recover its HM-phosphorylation. As seen in Fig 6E the mutant failed to display any detectable HM phosphorylation to establish that the 19 amino acid stretch independently mediated Torin sensitivity.

A novel eight amino-acid PHLPP1 binding region mediates S6K1 serum response.

Analysis of deletion variants described previously in their ability to regulate HM-phosphorylation in response to serum highlighted some interesting results. Deletion of a 13 amino acid stretch i.e. 78-90, from double truncation mutant of S6K1 conferred resistance to serum response, as the variant exhibited constitutive display of HM phosphorylation without discriminating between fasting and serum stimulated state (data not shown). Further analysis revealed that deletion of eight amino acid i.e.78-85 was sufficient to confer this resistance (Fig 7A). Next, we deleted this eight amino acid region from WTS6K1 to ascertain whether presence of TOS and CTD would influence phosphorylation dynamics of the mutant other than propagating negative regulation due to rapamycin. Surprisingly, the mutant continued to exhibit serum resistance (Fig 7B). The data further demonstrates that TOS-motif does not contribute in regulating serum response or HM-phosphorylation, but introduces rapamycin response. These observations therefore unequivocally associate TOS and CTD in propagating negative regulation.

In the backdrop of established relationship between HM-phosphorylation and its regulation by PHLPP1 (Pleckstrin Homology Domain Leucine-rich Repeat Protein Phosphatase(Liu et al., 2011)), we sought to examine whether the region that conferred serum resistance mediates any PHLPP1 dependence. Accordingly, the sequence segment (78-85), generated as a GST-fusion variant in pEBG vector was used as an affinity matrix for pull down assays using HEK293 cell extracts over expressing HA-PHLPP1. As seen in Fig 7C, the lane representing GST 78-85 was positive for HA-immunoblotting corresponding with PHLPP1 mobility. Expectedly, GST alone, negative for HA signal was suggestive that the sequence region mediated PHLPP1 binding. It was therefore plausible to assume that PHLPP1 binding dynamics must relate with serum response of S6K1. We therefore transfected HA- PHLPP1 in Flag-S6K1 HEK293 stable cell lines and examined changes, if any, in binding dynamics, with or without serum. Fig 7D clearly shows that PHLPP1 binding was significantly less in the presence of serum that corresponded with the state of HM-phosphorylation. This goes to indicate that serum response may be associated with loss of PHLPP1 binding to sustain phosphorylation at HM. In view of the recognized role of PHLPP1 in dephosphorylation and

inactivation of S6K1(Liu et al., 2011), we chose to evaluate whether S6K1 deletion variant (∆78-85), that exhibited serum resistance possibly for its inability to mediate PHLPP1 binding, would resist its PHLPP1 mediated inactivation. Accordingly, WT S6K1 and ∆78-85 variant were transfected with or without PHLPP1 to assess the state of their phosphorylation at HM. As seen in Fig 7E, while HM-phosphorylation in WT S6K1 was significantly lost in the presence of PHLPPL1, the deletion variant showed little or no loss of HM-phosphorylation/ activity to demonstrate PHLPP1 binding as a necessary attribute of serum response by S6K1.

Discussion

The nutrient-sensing attribute of mTORC1 coupled with its growth factor response presents an unusual example where negative and positive regulatory functions appear blended to display a cumulative response. However, our data provides a mechanism for S6K1 activation through stepwise action of mTOR complex1 and 2 and shows that the two processes work in tandem, where the quantum of nutrient availability serves to regulate the magnitude of stimulatory response in a rate-limiting manner.

Herein, we identify phosphorylated eIF4E as a mediator that transduces mTORC1 signals through its interaction with S6K1-TOS motif. The findings report eIF4E as an important determinant of cellular response to rapamycin in conformity with a long-standing contention that associates stoichiometric abundance of eIF4E with rapamycin resistance (Alain et al., 2012; Josse et al., 2016). Our earlier reports that identify eIF4E as a bonafide mTORC1 substrate(Batool et al., 2020) and factor responsible to propagate cellular response to rapamycin, serves to reinforce its prospect as an intermediate for S6K1 activation. The data further endorses the prevalence of enhanced eIF4E phosphorylation and S6K1 activation observed in several human cancers, including breast, gastric and colorectal tumours. However, the role of eIF4E phosphorylation in transducing mTORC1 signals has largely remained unexplored. This may be due to exclusive attribution of this phosphorylation to MNKs (Proud, 2015; Shveygert et al., 2010). Our data presented here that establishes mTORC1 as a primary eIF4E kinase and MNK1 as its feedback kinase, not only reconciles with the prospect of this phosphorylation in modulating mTORC1 response but also accounts for its role in propagating rapamycin resistance due to phosphorylation by MNK1. The attributes of eIF4E as a genuine mTORC1 effector are not only endorsed by its phosphorylation and faithful response to rapamycin *in vitro* and *in vivo* but also by its ability to bind raptor through a novel sequence motif (described previously by us as TPNPNPP(Batool et al., 2020)). Importantly, this sequence motif is conserved in most of the mTORC1 substrates other than S6K1 and 4EBP1. While the exclusion of these two proteins may not necessarily constitute a distinct class of mTORC1 substrates, instead, it may serve to represent a set of proteins that exhibit indirect regulation by mTORC1. This is consistent with a

reasonable amount of data, including our own, that advocates discordance between their phosphorylation turnover and the state of mTORC1 activation(Beigh et al., 2013; Showkat et al., 2014).

In conformity with our recent finding that suggests a possible interaction between eIF4E and S6K1(Batool et al., 2020), we herein show that eIF4E is a bonafide S6K1-TOS binding protein. A high quality prediction (RMSD<3.0) of TOS-eIF4E interaction, by flexible peptide-protein propensity modeling coupled with series of wet lab data, convincingly establish that TOS motif is indispensable for S6K1 to interact with phosphorylated eIF4E. Since eIF4E binding with S6K1 and its resultant activation remains rapamycin sensitive, we, therefore, conclude that the reports suggesting interaction of raptor with TOS motif appears to be a consequence of its engagement with eIF4E. Nonetheless, it was imperative to establish whether regulatory function of eIF4E resides in phosphorylation turnover of the protein per se or in its ability to proximate raptor-mTORC1 for S6K1 regulation. While we show that phosphorylation of eIF4E is sufficient to relieve S6K1 from rapamycin inhibition and its dependence on mTORC1, we further demonstrate that phospho-mimicked eIF4E (S209E) interacts with S6K1 even under raptor knockdown state. These observations dispel the notion that mTORC1 directly phosphorylates S6K1 at its hydrophobic motif. Instead, we conclude that mTORC1 effect is restricted to engagement of eIF4E with S6K1 to influence its state of HM phosphorylation and activation as a consequence. This engagement appears analogous to the role of eIF4E as a regulatory subunit that serves to overcome S6K1 inhibition due to nutrient deficiency etc. A significant body of literature endorses the view that this default inhibition is propagated by carboxy terminal auto inhibitory domain (CAD), which gets displaced upon TOS engagement(Weng et al., 1995; Weng et al., 1998). Accordingly, TOS dysfunction has been shown to be compensated by displacement/deletion of CAD to rescue HM phosphorylation with full activation of S6K1, regardless of the state of mTORC1 activation (Dennis et al., 2001). Taken together, these studies strengthen the contention that mTORC1 response propagated through eIF4E-TOS-CAD axis must serve to be rate limiting for the phosphorylation and activation of S6K1 by a kinase other than mTORC1.

In the backdrop of above results and established allegiance of S6K1 with AGC kinase(Powers, 2007), mTORC2 appears to have a natural stake as the potential kinase to phosphorylate HM of S6K1. While evidence of mTORC1 independent and Torin sensitive phosphorylation in several S6K1 mutants does support mTORC2 as a prospective S6K1 kinase (Ali and Sabatini, 2005), it has largely been ignored due to dogmatic kinship of S6K1 phosphorylation with mTORC1. In the context of our data that argues to replace raptor-mTORC1 recruitment view with eIF4E engagement model for mTORC1 independent phosphorylation, mTORC2 naturally assumes prominence as a potential HM

kinase. Further, the model is reasonably versed to explain the shortcomings that otherwise discredit mTORC2 as a favourable HM kinase. For example, rictor knockdown effect, in accordance with the view presented by us, can be appreciated in situations where inhibition due to CAD has been overcome, as seen in doubly truncated rapamycin resistant variant of S6K1.The wild type S6K1 must accordingly require priming due to TOS engagement before it begins to exhibit rictor knockdown response. This is further substantiated by the observation that ΔNHΔCT rather than wild type S6K1 serves as a better mTORC2 substrate during *in vitro* kinase assays (data not Shown). Notwithstanding the explanations, it was imperative to associate physiological specificity with the prospect of mTORC2 as a potential HM kinase of S6K1. An elaborate deletion analysis identifies a 19 amino acid- pleated stretch (91-109) responsible for mediating HM phosphorylation by a Torin sensitive kinase and weakens the notion of the event being random. Furthermore, loss of HM phosphorylation in S6K1 variant deleted off this 19 amino acid stretch, despite the presence of a consensus TOS motif, unequivocally implicates the region in mediating HM phosphorylation. Although, we do not demonstrate a direct interaction between this 19 amino acid region and mTORC2, we do propose that this region serves as a landing site for mTORC2 or a kinase regulated by it in a Torin dependent manner. We have, in a separate study, observed enhanced S6K1 phosphorylation/activation upon over expression of AMPK 1 subunit (data not shown). In conformity with the established data(Jacinto, 2019; Kazyken et al., 2019), overexpression of AMPK α1 subunit also caused mTORC2 activation. An interesting deduction from these observations was that AMPK could override the inhibitory effects of caffeine (a reported inhibitor of mTORC2(Grant et al., 2012; Tariqul Islam et al., 2019)) on S6K1, it however, did not alter rapamycin inhibition. These data further strengthen the role of mTORC2 as a bonafide HM kinase for S6K1. Taken together, these observations clearly support our view that mTOR complex 1 and 2 responses are required in tandem to bring about complete S6K1 activation.

Functional analysis of deletion mutants of S6K1 reveal a sequence segment of eight amino acids (78-85) that mediates its response towards serum. While deletion of this sequence renders S6K1 non responsive to serum stimulation, it does not affect its sensitivity towards rapamycin. The observation further substantiates our contention that mTORC1 response and HM phosphorylation are mutually exclusive events. We further show that this eight amino acid stretch is a PHLPP1 binding region and serum stimulation of cells dislodges PHLPP1 to allow full activation of S6K1. These results, thus, add another dimension to S6K1 activation, where HM phosphorylation is also regulated by the dynamics of phosphatase binding. Taken together, the data is summed up in the form of a schematic model (Figure 8) that describes mTORC1 phosphorylated eIF4E, mTORC2 and

PHLPP1 as participant regulators of S6K1. The model, hence, provides a mechanism for how stepwise contribution of these participants bring about complete activation S6K1.

Materials and Methods

Cell lines and Culture Conditions

HEK293 were a gift from Dr.Tyagi JNU-India. HEK293T and NIH3T3 were gifted by Dr. Fayaz Malik and Dr. Jamal respectively (CSIR-IIIM Jammu). A549, MCF-7, MDA-MB and HCT were purchased from NCCS, Pune-India. The cell lines were maintained in Dulbecco's modified Eagles medium (DMEM) supplemented with 10% (v/v) fetal bovine serum (Invitrogen), 50 µg/ml penicillin and 100 µg/ml streptomycin (Sigma-Aldrich) at 37°C with 5% CO_2. The experiments where select inhibitors were used had the growing cells plated at $3*10^5$ cells per ml density prior to their treatment and incubation for variable time points at 37^oC with 5% CO_2, before harvesting for further analysis.

Chemicals and Antibodies

PVDF membrane (GE Healthcare/Millipore), Rapamycin (Sigma Aldrich) and Mnk1 inhibitor (Merck USA), Protein G-Agarose beads (Genscript), Torin (Tocris), Glutathione agarose beads (Thermo-scientific). Polyetheleneimine reagent (Polysciences, Inc.), Radioactive ATP (BRIT, Hyderabad-India). Antibodies against p-S6K1(T389/T412), p-eIF4E(S209), mTOR, Raptor, ULK1, S6, Flag-tag were bought from Cell Signaling Technologies (Beverly MA); HA-tag, myc-tag, tubulin, GST and GAPDH (Sigma-Aldrich); 4E-BP1 and eIF4E (Abcam); β-actin (Thermo Scientific), rabbit and mouse secondary antibodies conjugated to IR Dye 800CW (LI-COR Biotechnology, Lincoln, Nebraska); S6K1 (GenScript)

Expression Vectors and Transfections

A cDNA plasmid encoding HA-PHLPP1 was received as a gift from Dr. Alexandra Newton, University of California, Sandiego. A pMT2-based cDNA encoding an amino-terminal HA-tagged S6K1 (αI variant) and its truncation mutants S6K1ΔCT, S6K1ΔNH, S6K1ΔNH-ΔCT were kindly gifted by Prof. Joseph Avruch, Harvard Medical School Boston, USA. S6K1 point mutant S6K1412E, described previously (Beigh et al., 2013) served as a template to construct NH(2-46)T412E mutant. The primers used were (1) 5'GAGAATTCATGGGGGGTCAGTTAAATG and (2) 5'GCCGAATTCTCATAGATTCATACGCAGGTGC. The primers were annealed and inserted into EcoRI digested HA-tagged S6K1 construct. cDNA clones of HA-ULK1 (plasmid#31963), HA-eIF4E (plasmid#17343), HA-Raptor (#8513), myc-kinase dead mTOR (#8482), myc-mTOR (#1861), pEBG (#22227) and myc-PRAS40 (#15476) were purchased from addgene. HA tagged ULK1 truncation mutant ULK1Δ401-407 was generated using primers (1) 5'Phos-TGCAGCAGCTCCCCCAGTCCCTCAGGCCGG and (2) 5'Phos-

CCGGCCGTGGCTCTCCAAGCCCGCAGAGGC. HA-tagged eIF4E, previously sub-cloned in pKMYC vector backbone(Batool, A.; Majeed, S.T.; Aashaq, S.; Majeed, R.; Shah, G.; Nazir, N.; Andrabi, 2019), was used as template to generate its truncation variant, eIF4E∆9-15. Following primers were used for the purpose (1) 5'Phos-ACTACAGAAGAGGAGAAAACGGAATC and (2) 5'Phos- GGTTTCCGGTTCGACAGTCGCCAT. Phospho deficient mutant of eIF4E, S209A was constructed using primers (1) 5′GCTACTAAGAGCGGCGCCACCACTAA (2) 5′ TATTTTTAGTGGTGGCGCCGCTCTTAG while as its phosphomimicked variant, S209E was constructed using primers (1) 5' GCTACTAAGAGCGGCGAGACCACTAA (2) 5' CGCGCGAATTCTTAAACAACAAACCTATT respectively. Myc tagged PRAS40 truncation mutant ∆88-94 truncation mutant was generated by using primers (1) 5'Phos-CGGCCTACCCTGGCCAGAGAGGA and (2) 5'Phos- GGGTGGCTGTGGTGCTGGTGGGG. The mutations were verified by DNA sequence and restriction analysis. For transient transfection of cells, 1×10^6 cells were plated onto a 60-mm dish 24 hr prior to transfection. 1-2 µg of Plasmid DNA along with transfection agents Lipofectamine (Invitrogen) or Plyetheleneimoine, PEI (Polysciences, Inc.) were used to transfect the cells. Standard protocol was followed for cell transfection. Stable cell lines of HEK293 overexpressing S6K1 were generated by retroviral transduction of pWZL-Neo-Myr-Flag-RPS6KB1 plasmid, purchased from addgene (#20624), selected and maintained with neomycin (500 µg/ml).

Gene Knock Down using shRNA

Lentiviral shRNA plasmid against MNK1 was a kind gift from Dr. Ronald. B. Gartenhaus (University of Maryland Baltimore, USA). Vector containing the appropriate shRNA i.e. non-target shRNA (SHC002) was purchased from Sigma Aldrich while shRNA to human raptor (plasmid#1857), mTOR (plasmid#1855) were purchased from Addgene. eIF4E shRNA (plasmid 35284-SH) and 4E-BP1 shRNA (plasmid 29594-SH) were purchased from Santa Cruz. The plasmids were separately co-transfected into HEK293T packaging cells along with pCMV-dR 8.2 dvpr and pCMV-VSV-G using PEI reagent. 48hrs post transfection, medium containing lentiviral particles was filtered, collected and used to infect HEK293 cells in presence of polybrene (8µg/ml). Viral particles containing medium was removed 48 hrs post infection and replaced with fresh medium containing 2.5ug/ml of puromycin for selection of transduced cells for 5 days. Surviving colonies were allowed to grow for 2 weeks and were then ring-cloned and placed in 6cm plates in 3 ml of medium containing 10% FBS, and 2µg/ml puromycin. Ten colonies were selected for further evaluation.

Immuno-precipitations and Western blotting

48 h post transfection, cells were starved overnight in serum-free DMEM. Cells were serum stimulated for 30 minutes in presence or absence of rapamycin (50nM) or Torin (50nM) as per the

experimental requirements before lysis with ice cold CHAPS lysis buffer (Kim et al., 2002) MNK1 inhibitor, (CAS-522629), at a final concentration of 5-30µM was used 60 hours post transfection. Centrifugation (micro centrifuge, 13,000 rpm at 4°C for 20 min) was carried out to remove the precipitated material and cleared lysates obtained were incubated overnight with appropriate antibody immobilized on protein G-Agarose beads. Beads were washed five times with CHAPS lysis buffer. Laemmli sample buffer was added to the beads, which were then subjected to SDS-PAGE. Proteins were transferred on PVDF membrane, probed with different antibodies at indicated concentrations and analyzed using Odyssey infrared imager (LI-COR).

***In vitro* kinase assay**

In Vitro Kinase assay has been described previously(Batool et al., 2020; Beigh et al., 2012). Briefly, Proteins immobilized on either HA or Myc-beads were incubated with 1µg of the substrate and 5µCi ^{32}PATP in a kinase reaction buffer containing 50mM Tris-Cl (pH 7.0), 10mM MgCl2, 0.5mM DTT, 50mM β-Glycero-phosphate, and 1mM ATP for 15 minutes at 37°C.Reaction was stopped by adding 5X loading buffer, run on an SDS-PAGE gel. Proteins were transferred on PVDF membrane, auto-radiographed and activity determined by standard protocol.

Protein extraction from Tissues

Tissue (100mg) was immersed in 0.5% trypsin-EDTA (warm solution) and incubated at 37°C for 5 minutes, washed with ice-cold PBS, and incubated with lysis buffer (50 mM Tris–Cl (pH 7.5), 10 mM MgCl2, 5 mM EDTA, 2 mM DTT, 50 Mm β-Glycero-phosphate, 0.5% Triton X-100 and Protease inhibitor cocktail) for 30min followed by centrifuge at 4˚c at 10,000 rpm for 45 min. The tissue was vortexed after every 10 min. The supernatant containing protein was collected.

Statistical Analysis

Statistical analysis was performed using GraphPad software (Prism 8). All error bars represent SEM. For multiple group comparisons all groups from each experimental repeat were compared using ANOVA. If the ANOVA test was significant ($p < 0.05$), Tukey's test was performed. Pearson r analysis was used for data comparing only two groups. All asterisks denote a significant p value defined * for $P < 0.05$ and ** for $P <0.01$.

Acknowledgement

We are thankful to Dr. Joseph Avruch from Mass.General Hospital, Harvard Medical School, Boston-MA, Dr. Ronald B. Gartenhaus from University of Maryland, Baltimore, Maryland, Dr. Alexandra C. Newton from University of California, Sandiego for generously sharing important reagents. We also thank Dr. Shazia Irshad from Nuffield Department of clinical laboratory sciences, University of Oxford for editing the manuscript. Fellowships in favor of S.T.M and R.M from University Grants Commission (UGC) under CPEPA (2-5/2016(NS/PE) and financial support by DST-SERB

(EMR/2016/000803), DBT (BT/PR5867/BRB/10/1107/2012) and University Grants Commission CPEPA (2-5/2016(NS/PE) are duly acknowledged.

Author Contributions

S.T.M. designed and performed the experiments, generated S6K1 stable and mTOR, MNK1, rictor knock down cell lines, constructed S6K1 mutants, analysed and interpreted the data and wrote the manuscript. A.B. extracted proteins from cancer and normal tissues, constructed eIF4E mutants and generated 4EBP1 knock down cells. R.M. constructed ULK1 and PRAS40 mutants, generated Raptor knockdown cells lines. N.N.B. performed bioinformatics analysis. KIA conceived and supervised the project, designed the experiments, interpreted the data and wrote the manuscript.

Declaration of Interests

The authors declare no competing interests.

References

Alain, T., Morita, M., Fonseca, B. D., Yanagiya, A., Siddiqui, N., Bhat, M., Zammit, D., Marcus, V., Metrakos, P., Voyer, L. A., et al. (2012). eIF4E/4E-BP ratio predicts the efficacy of mTOR targeted therapies. *Cancer Res.* **72**, 6468–6476.

Ali, S. M. and Sabatini, D. M. (2005). Structure of S6 kinase 1 determines whether raptor-mTOR or rictor-mTOR phosphorylates its hydrophobic motif site. *J. Biol. Chem.* **280**, 19445–19448.

Batool, A., Majeed, S. T., Aashaq, S., Majeed, R., Bhat, N. N. and Andrabi, K. I. (2020). Eukaryotic initiation factor 4E is a novel effector of mTORC1 signaling pathway in cross talk with Mnk1. *Mol. Cell. Biochem.* **465**, 13–26.

Batool, A.; Majeed, S.T.; Aashaq, S.; Majeed, R.; Shah, G.; Nazir, N.; Andrabi, K. I. (2019). Eukaryotic Initiation Factor 4E (eIF4E) sequestration mediates 4E-BP1 response to rapamycin. *Int J Biol Macromol* **125**, 651–659.

Beigh, M. A., Showkat, M., Ul Hussain, M., Latoo, S. A., Majeed, S. T. and Andrabi, K. I. (2012). Rapamycin inhibition of baculovirus recombinant (BVr) ribosomal protein S6 kinase (S6K1) is mediated by an event other than phosphorylation. *Cell Commun. Signal.* **10**,.

Beigh, M. A., Showkat, M., Hussain, M. U. and Andrabi, K. I. (2013). Loss of hydrophobic motif and activation loop phosphorylation is a consequence and not the mechanism of S6 kinase 1 inhibition by rapamycin. *J. Biol. Regul. Homeost. Agents* **27**, 399–408.

Ben-Hur, V., Denichenko, P., Siegfried, Z., Maimon, A., Krainer, A., Davidson, B. and Karni, R.

(2013). S6K1 Alternative Splicing Modulates Its Oncogenic Activity and Regulates mTORC1. *Cell Rep.* **3**, 103–115.

Brown, M. C. and Gromeier, M. (2017). MNK Controls mTORC1:Substrate Association through Regulation of TELO2 Binding with mTORC1. *Cell Rep.* **18**, 1444–1457.

Dennis, P. B., Jaeschke, A., Saitoh, M., Fowler, B., Kozma, S. C. and Thomas, G. (2001). Mammalian TOR: A homeostatic ATP sensor. *Science (80-.).* **294**, 1102–1105.

García-Martínez, J. M. and Alessi, D. R. (2008). mTOR complex 2 (mTORC2) controls hydrophobic motif phosphorylation and activation of serum- and glucocorticoid-induced protein kinase 1 (SGK1). *Biochem. J.* **416**, 375–385.

Grant, I., Cartwright, J. E., Lumicisi, B., Wallace, A. E. and Whitley, G. S. (2012). Caffeine inhibits EGF-stimulated trophoblast cell motility through the inhibition of mTORC2 and Akt. *Endocrinology* **153**, 4502–4510.

Hong, S., Freeberg, M. A., Han, T., Kamath, A., Yao, Y., Fukuda, T., Suzuki, T., Kim, J. K. and Inoki, K. (2017). LARP1 functions as a molecular switch for mTORC1-mediated translation of an essential class of mRNAs. *Elife* **6**,.

Ito, H., Ichiyanagi, O., Naito, S., Bilim, V. N., Tomita, Y., Kato, T., Nagaoka, A. and Tsuchiya, N. (2016). GSK-3 directly regulates phospho-4EBP1 in renal cell carcinoma cell-line: An intrinsic subcellular mechanism for resistance to mTORC1 inhibition. *BMC Cancer* **16**,.

Jacinto, E. (2019). Amplifying mTORC2 signals through AMPK during energetic stress. *Sci. Signal.* **12**,.

Josse, L., Xie, J., Proud, C. G. and Smales, C. M. (2016). mTORC1 signalling and eIF4E/4E-BP1 translation initiation factor stoichiometry influence recombinant protein productivity from GS-CHOK1 cells. *Biochem. J.* **473**, 4651–4664.

Kazyken, D., Magnuson, B., Bodur, C., Acosta-Jaquez, H. A., Zhang, D., Tong, X., Barnes, T. M., Steinl, G. K., Patterson, N. E., Altheim, C. H., et al. (2019). AMPK directly activates mTORC2 to promote cell survival during acute energetic stress. *Sci. Signal.* **12**,.

Kim, D. H., Sarbassov, D. D., Ali, S. M., King, J. E., Latek, R. R., Erdjument-Bromage, H., Tempst, P. and Sabatini, D. M. (2002). mTOR interacts with raptor to form a nutrient-sensitive complex that signals to the cell growth machinery. *Cell* **110**, 163–175.

Kim, J., Kundu, M., Viollet, B. and Guan, K. L. (2011). AMPK and mTOR regulate autophagy through direct phosphorylation of Ulk1. *Nat. Cell Biol.* **13**, 132–141.

Koren, I., Reem, E. and Kimchi, A. (2010). DAP1, a novel substrate of mTOR, negatively regulates autophagy. *Curr. Biol.* **20**, 1093–1098.

Kurcinski, M., Jamroz, M., Blaszczyk, M., Kolinski, A. and Kmiecik, S. (2015). CABS-dock web

server for the flexible docking of peptides to proteins without prior knowledge of the binding site. *Nucleic Acids Res.* **43**, W419–W424.

Li, P. D., Zhang, W. J., Zhang, M. Y., Yuan, L. J., Cha, Y. L., Ying, X. F., Wu, G. and Wang, H. Y. (2012). Overexpression of RPS6KB1 predicts worse prognosis in primary HCC patients. *Med. Oncol.* **29**, 3070–3076.

Liu, J., Stevens, P. D., Li, X., Schmidt, M. D. and Gao, T. (2011). PHLPP-Mediated Dephosphorylation of S6K1 Inhibits Protein Translation and Cell Growth. *Mol. Cell. Biol.* **31**, 4917–4927.

Majeed, S.T.; Majeed, R.; Shah, G.; Andrabi, K. I. (2019). S6 Kinase: A Compelling Prospect for Therapeutic Interventions. In *Homeostasis-An Integrated Vision* (ed. Castanho, F.L.; Garnes, S. D. A.), pp. 143–162. Intech.

Martín, M. E., Pérez, M. I., Redondo, C., Álvarez, M. I., Salinas, M. and Fando, J. L. (2000). 4E binding protein 1 expression is inversely correlated to the progression of gastrointestinal cancers. *Int. J. Biochem. Cell Biol.* **32**, 633–642.

Nojima, H., Tokunaga, C., Eguchi, S., Oshiro, N., Hidayat, S., Yoshino, K. I., Hara, K., Tanaka, N., Avruch, J. and Yonezawa, K. (2003). The mTOR partner, Raptor binds the mTOR substrates, p70 S6 kinase and 4E-BP1 through their TOS (TOR signaling) motif. *J Biol Chem*.

Powers, T. (2007). TOR Signaling and S6 Kinase 1: Yeast Catches Up. *Cell Metab.* **6**, 1–2.

Proud, C. G. (2015). Mnks, eIF4E phosphorylation and cancer. *Biochim. Biophys. Acta - Gene Regul. Mech.* **1849**, 766–773.

Saxton, R. A. and Sabatini, D. M. (2017). mTOR Signaling in Growth, Metabolism, and Disease. *Cell* **168**, 960–976.

Schalm, S. S. and Blenis, J. (2002). Identification of a conserved motif required for mTOR signaling. *Curr. Biol.* **12**, 632–639.

Schalm, S. S., Fingar, D. C., Sabatini, D. M. and Blenis, J. (2003). TOS motif-mediated raptor binding regulates 4E-BP1 multisite phosphorylation and function. *Curr. Biol.* **13**, 797–806.

Showkat, M., Beigh, M. A., Bhat, B. B., Batool, A. and Andrabi, K. I. (2014). Phosphorylation dynamics of eukaryotic initiation factor 4E binding protein 1 (4E-BP1) is discordant with its potential to interact with eukaryotic initiation factor 4E (eIF4E). *Cell. Signal.* **26**, 2117–2121.

Shveygert, M., Kaiser, C., Bradrick, S. S. and Gromeier, M. (2010). Regulation of Eukaryotic Initiation Factor 4E (eIF4E) Phosphorylation by Mitogen-Activated Protein Kinase Occurs through Modulation of Mnk1-eIF4G Interaction. *Mol. Cell. Biol.* **30**, 5160–5167.

Siddiqui, N. and Sonenberg, N. (2015). Signalling to eIF4E in cancer. *Biochem. Soc. Trans.* **43**, 763–772.

Stead, R. L. and Proud, C. G. (2013). Rapamycin enhances eIF4E phosphorylation by activating MAP kinase-interacting kinase 2a (Mnk2a). *FEBS Lett.* **587**, 2623–2628.

Tariqul Islam, A. F. M., Scavello, M., Lotfi, P., Daniel, D., Haldeman, P. and Charest, P. G. (2019). Caffeine inhibits PI3K and mTORC2 in Dictyostelium and differentially affects multiple other cAMP chemoattractant signaling effectors. *Mol. Cell. Biochem.*

Wendel, H. G., Silva, R. L. A., Malina, A., Mills, J. R., Zhu, H., Ueda, T., Watanabe-Fukunaga, R., Fukunaga, R., Teruya-Feldstein, J., Pelletier, J., et al. (2007). Dissecting eIF4E action in tumorigenesis. *Genes Dev.* **21**, 3232–3237.

Weng, Q. P., Andrabi, K., Kozlowski, M. T., Grove, J. R. and Avruch, J. (1995). Multiple independent inputs are required for activation of the p70 S6 kinase. *Mol. Cell. Biol.* **15**, 2333–2340.

Weng, Q. P., Kozlowski, M., Belham, C., Zhang, A., Comb, M. J. and Avruch, J. (1998). Regulation of the p70 S6 kinase by phosphorylation in vivo. Analysis using site-specific anti-phosphopeptide antibodies. *J. Biol. Chem.* **273**, 16621–16629.

Yang, H., Jiang, X., Li, B., Yang, H. J., Miller, M., Yang, A., Dhar, A. and Pavletich, N. P. (2017). Mechanisms of mTORC1 activation by RHEB and inhibition by PRAS40. *Nature* **552**, 368–373.

Yip, C. K., Murata, K., Walz, T., Sabatini, D. M. and Kang, S. A. (2010). Structure of the Human mTOR Complex I and Its Implications for Rapamycin Inhibition. *Mol. Cell* **38**, 768–774.

Zhang, S., Hu, B., Lv, X., Chen, S., Liu, W. and Shao, Z. (2019). The prognostic role of ribosomal protein S6 kinase 1 pathway in patients with solid tumors: A meta-analysis. *Front. Oncol.* **9**,.

Legends

Fig 1. eIF4E phosphorylation governs S6K1 activation state.

(A and B) Expression pattern of eIF4E and S6K1 in cancer cells and tissues.

Breast cancer (MCF7, MDA-MB28), Lung Cancer (A549) Colon Cancer (HCT) cells along with non-transformed HEK293, NIH3T3 (A) or representatives from Breast, Gastric, Colorectal cancer tissues (represented as T) along with their adjacent normal tissues (represented as N) (B) were harvested and analyzed by immunoblots using indicated antibodies. Quantitation represents the average of three independent experimental series normalized to actin control. Error bars denote SEM.

(C and D) Phosphorylation levels of eIF4E and S6K1 in cancer tissues and Cell lines.

The lysates of cell lines and tissues described in A and B, were analysed by immunoblot as shown. To ensure that increase in the phosphorylation levels is not due to increased total protein levels in cancer samples, total protein load was optimized to bring eIF4E and S6K1 protein levels in cancer samples at par with their corresponding control samples. Unequal loading pattern is seen due to this optimization. Quantitation showing eIF4e and S6K1 phosphorylation levels represents average results of three independent experimental series normalized to their respective protein content. Error bars denote SEM.

(E and F) eIF4E abundance enhances S6K1 activation.

NIH3T3, HEK293 cells transfected with myc-eIF4E (C) or HEK293 cells infected with 4EBP1 or scrambled shRNA (D) were each grown in three 90mm culture dishes. The lysate from each set was pooled such as to increase the levels of S6K1 in each lysate. The lysates were subjected to endogenous S6K1 IP to monitor S6K1 activity. S6K1 kinase activity was monitored using GST-S6 as a substrate. Immunoblots represent levels of indicated proteins.

(G) Phosphorylation state of eIF4E governs S6K1 activity

Flag-S6K1 stable HEK293 cells lines transfected with myc-eIF4E or its Phospho mimicked (S209E) or phosphodeficient (Ser209A) were lysed directly or after 30 min incubation with 50nM rapamycin. The lysates obtained were Flag Immunoprecipitated. S6K1 activity was monitored as described in (E and F).The immunoblots were probed with indicated antibodies.

Fig 2. mTORC1 interacts with and phosphorylates eIF4E

(A and B) eIF4E phosphorylation is responsive towards mTORC1 input.

Serum-stimulated Flag-S6K1 stable HEK293 cells were either lysed directly or after incubation with agents known to inhibit mTORC1 input (100 mM 2-Deoxy Glucose or 20 mM rotenone or 50nM rapamycin for 30 minutes). Alternatively, mTORC1 inhibition was achieved by growing cells in amino acid free media (EBSS). The lysates obtained were immunoblotted and analyzed for phospho-eIF4E levels (A). HEK293 cells were infected either with mTOR or raptor shRNAs to generate respective knockdown cell lines. Scrambled shRNA was used as control. Additionally, 1 µg each of myc-mTOR and HA-raptor encoding plasmids were respectively transfected in mTOR and raptor shRNA cell lines to rescue their knock down effects. The cells were grown in serum supplemented DMEM media for 60 hours after transfection. Cells were lysed in ice cold lysis buffer. The lysates obtained were immunoblotted and analyzed for phospho-eIF4E levels (B).

(C and D) eIF4E interacts with mTORC1 adaptor protein, raptor.

HA-Raptor and myc-eIF4E interact in transfected HEK293 cells. Shown are the levels of myc-eIF4E (top) and HA-Raptor and myc- tubulin (middle) in anti- HA immunoprecipitates prepared from HEK293 cells transfected with 1 µg of a plasmid encoding myc-eIF4E and 1 µg of one encoding either HA- Raptor or HA- tubulin (C). Endogenous Raptor (top) interacts with HA-eIF4E but not tubulin (bottom). Anti-HA immunoprecipitates were prepared from HEK293T cells transfected with 1 µg of either HA-eIF4E or HA-tubulin encoding plasmid (D).

(E-G) eIF4E and other mTORC1 substrates interact with raptor through a novel consensus sequence motif.

Representation of a novel raptor binding motif present across various mTORC1 substrates (E).Flexible protein peptide docking conducted through CABS-doc webserver represents the binding potential of the raptor with sequence motifs corresponding to ULK1, eIF4E, PRAS40 and LARP1 (F). HEK293T cells were transfected with Wild type myc-eIF4E, myc-PRAS40, HA-ULK1 and their truncation mutants, lacking potential raptor binding region. 60 hours post transfection, cells were lysed and the lysates obtained were subjected to myc and HA IP, as indicated and analyzed for endogenous raptor levels (G).

Fig 3: MNK mediated eIF4E Phosphorylation is a rapamycin activated feedback response

(A) Assessment of MNK1 kinase activity state in cancer and non-transformed cell lines.
Indicated cancer cell lines and non-transformed HEK293 and NIH3T3 cells were grown in 90mm culture dishes, lysed and MNK1 immunoprecipitated. MNK1 kinase activity was monitored by using GST-4E as a substrate. Quantitation represents average results of three independent experimental series. Error bars denote SEM.
(B) Effect of MNK1 inhibitor (CGP57380), used in indicated concentrations and for indicated time periods, was assessed on the kinase activity of MNK1, extracted from NIH3T3 and MCF7 cell lines as described in (A). Quantitation represents average results of three independent experimental series.
(C, D) MNK1 is not the primary kinase for eIF4E
Cell lysates obtained from indicated cell lines were treated with CGP57380 (10µM) and rapamycin (50nM) for 30 minutes prior to lysis. The lysates were immunoblotted and analyzed for phospho-eIF4E levels (C). HEK293 cells were infected with MNK1 shRNAs to generate MNK1 knockdown cell line. Scrambled shRNA was used as control. Additionally, 1 µg each of HA-MNK1 encoding plasmid was transfected in MNK1shRNA cell line to rescue its knock down effect. The cells were grown in serum supplemented DMEM media for 60 hours after transfection. Cells were lysed in ice cold lysis buffer. The lysates obtained were immunoblotted and analyzed for phospho-eIF4E levels (D).
(E-F) MNK1 is a feedback kinase for eIF4E.
HEK293T cell lines were treated with 250nM rapamycin for indicated time periods before lysis. The lysates were immunoblotted and analyzed for phospho-eIF4E levels (E). HEK293 cells were infected with control or MNK1 shRNA as described in (D). Prior to lysis, the cells were treated with 50 nM rapamycin for 12 hours. The lysates obtained were assed for phospo-eIF4E levels (F).

Fig 4. eIF4E interacts with TOS motif of S6K1

(A) eIF4E-S6K1 interaction does not depend on the activity state of S6K1.
HA tagged WTS6K1, its phospho-mutant forms, S6K1T412A and S6K1T412E and Tubulin (serving as negative control) were co-transfected with myc-eIF4E in HEK293 cells. 60 hours post transfection, cells were lysed, HA immunoprecipitated and immunoblotted. The immunoblots were analysed for eIF4E levels.
(B-D) eIF4E binds TOS motif of S6K1.
HA tagged WTS6K1 alongside its point mutants F28A and F16A were transfected in HEK293T cells. The cells were grown in serum supplemented DMEM for 60 hours after transfection. Cells were lysed and the lysates were subjected to HA immuno-precipitation and immunoblotting. The immunoblots were analysed for endogenous levels of eIF4E (B).Flexible protein peptide docking conducted through CABS-doc webserver represents the binding potential of the eIF4E with TOS motifs of S6K1 and 4EBP1 (C). Flag-S6K1 stable HEK293 cells were transfected with myc-eIF4E. 60 hours post transfection, cells were lysed and lysates were subjected to myc IP. Prior to immunoblotting, increasing concentrations of intact (FDIDL) or disrupted (ADIDL) TOS peptides were added to the immunoprecipitates in indicated manner. The immunoblots were probed for the levels of S6K1 (D).
(E, F) Raptor does not mediate eIF4E-S6K1 interaction.
HEK293 cells were infected with raptor shRNAs to generate raptor knockdown cell line. Scrambled shRNA was used as control. The cells were transfected with myc tagged WT-eIF4E, its phospho-mutants, and tubulin (serving as negative control). Additionally, 1 µg of HA-raptor encoding plasmid was transfected in raptor shRNA cell line to rescue its knock down effect. The cells were grown in serum supplemented DMEM for 60 hours after transfection. Cells were lysed in ice cold lysis buffer, subjected to myc-IP and immunoblotted. The immunoblots were analyzed for S6K1 levels (E).Flag-S6K1 stable cell lines were transfected with eIF4E variant 30-217, its phosphodeficient and phosphomimicked variants. 60 hours post transfection, cells were lysed and subjected to myc-IP and immunoblotting. The immunoblots were analysed for the levels of S6K1 (F).

Fig 5. eIF4E-TOS interaction primes S6K1 for mTORC2 mediated activation.

(A) Phosphorylation at T412 site does not compensate for TOS dysfunction.

HEK293 cells were transfected in indicated manner with HA tagged WTS6K1 and ∆NHS6K1 and their phosphomimicked (T412E) variants. 60 hours post transfection, cells were lysed and subjected to HA-IP to monitor S6K1 activity. S6K1 kinase activity was monitored using GST-S6 as a substrate in an *in vitro* kinase assay. The immunoblot represents levels of indicated proteins.

(B, C) TOS motif relieves S6K1 from inhibition caused by carboxy terminus.

HEK293 cells transfected with HA tagged WTS6K1, TOS mutant (F28A) and carboxy terminus deleted variant of TOS mutant (F28A ∆CT), were grown in serum supplemented DMEM for 48 hours and then serum starved for 12 hours. Prior to lysis, cells were serum stimulated for 30 minutes directly or in presence of 50 nM rapamycin. The lysates were HA immunoprecipitated to monitor the S6K1 activity. The immunoblot was further analyzed for T412 phosphorylation levels of S6K1 (B). HEK293 cells were transfected with HA tagged WTS6K1 and truncation mutant lacking amino and carboxy termini (∆NH∆CT). The cells were grown in serum-supplemented DMEM for 60 hours. Cells were either lysed directly or after incubation with agents known to inhibit mTORC1 input (100 mM 2-Deoxy Glucose or 50nM rapamycin for 30 minutes). Alternatively, mTORC1 inhibition was achieved by growing cells in amino acid free media (EBSS). The lysates obtained were HA immunoprecipitated and subjected to *in vitro* kinase assay to monitor S6K1 activity. GST-S6 was used as substrate. The immunoblot represents the levels of indicated proteins.

(D-F) mTORC2 mediates S6K1 hydrophobic motif phosphorylation.

HEK293 cells transfected with HA tagged WTS6K1 and ∆NH∆CTS6K1 were either lysed directly or after treatment with 50nM Torin. The lysates were HA immunoprecipitated to monitor HM phosphorylation levels and S6K1 activity (D). HEK293 cells were infected with rictor shRNA to generate rictor knockdown cell line. Scrambled shRNA was used as control. The cells were transfected with HA tagged WT-S6K1 and ∆NH∆CTS6K1 and grown in serum supplemented DMEM for 60 hours. Cells were either lysed directly or after 30 minutes of incubation with 50nM of Rapamycin or Torin. The lysates were HA immnuno precipitated and analyzed for T412 phosphorylation levels of S6K1 (E). Rictor or scrambled shRNA infected HEK393 cells were transfected with HA-WTS6K1. Additionally, 1 µg of myc-rictor encoding plasmid was transfected in rictor shRNA cell line to rescue its knock down effect. Transfected cells were grown in serum supplemented DMEM for 48 hours and then serum starved for 12 hours. Cells were either lysed directly or after 30 minutes of serum stimulation. The lysates were HA immunoprecipitated and immunoblotted for detecting the T412 phosphorylation levels of S6K1 present in hydrophobic motif (F).

Fig 6. A 19 amino acid stretch is responsible for mediating mTORC2 response.

(A) Presence of a consensus TOS motif sequence in catalytic domain of S6K1.

(B) Amino acid sequence alignment of random loop of S6K1 connecting its amino terminus with catalytic domain.

(C-E) A 19 amino acid stretch mediates mTORC2 response.

HEK293 cells were transfected with indicated mutants of HA tagged S6K1. The cells were grown in serum supplemented DMEM for 60 hours. Cells were lysed and subjected to HA IP to monitor the S6K1 activity using GST-S6 as substrate. The immunoblots were further analyzed for detecting the T412 phosphorylation levels of S6K1 present in HM (C, D). HA tagged WTS6K1 and its truncation variant (∆91-109) were transfected in HEK293 cells. The S6K1 activity and HM phosphorylation was monitored (E).

Fig 7. A novel eight amino-acid PHLPP1 binding region of S6K1 mediates serum response.

(A, B) Eight Amino acid stretch of S6K1 mediates serum response.

HEK293 cells were transfected with indicated truncation mutants of S6K1. Cells were grown in serum supplemented media for 48 hours and then serum starved for 12 hours. Prior to lysis, cells were serum stimulated for 30 minutes, as indicated. The lysates were HA immunoprecipitated to monitor the S6K1 hydrophobic motif phosphorylation and its kinase activity. S6K1 kinase activity was monitored using GST-S6 as a substrate. Further, the ∆immunoblots were analyzed for indicated proteins.

(C) PHLPP1 binds to eight amino acid stretch of S6K1.

Glutathione agarose beads were used to pull down GST alone and or GST tagged S6K1 fragment (78-85) from transfected HEK293 cells. The beads were then incubated with HEK293 lysates containing HA-PHLPP1 and or HA-Tubulin and subjected to immnuno-blotting. The immnuno-blots were analyzed for PHLPP1 binding.

(D, E) Serum response of S6K1 is associated with loss of PHLPP1 binding.

Flag S6K1 stable HEK293 cells were transfected with HA tagged PHLPP1 or Tubulin (serving as a negative control) and grown in serum supplemented DMEM for 48 hours. The cells were then serum starved for 12 hours. Prior to lysis, cells were serum stimulated for 30 minutes. The lysates obtained were subjected to Flag IP and immunoblotting. The immunoblots were probed by anti HA antibody to monitor the levels of PHLPP1 in basal and serum stimulated state.

(E) PHLPP1 binding region of S6K1 mediates serum response.

HEK293 cells were transfected with HA tagged WTS6K1 or ∆78-85S6K1 (PHLPP1 binding deletion mutant) alone or alongside HA-PHLPP1. The cells were grown in 90mm culture dishes in serum supplemented media for 48 hours and then serum starved for 12 hours. The cells were then lysed and subjected to endogenous S6K1 IP and immunoblotted. The immunoblots were probed for observing changes in HM phosphorylation and kinase activity of S6K1 in its Wild type and mutant form.

Fig 8: Graphical illustration, describing mTORC1 phosphorylated eIF4E, mTORC2 and PHLPP1 as participants for complete activation of S6K1.

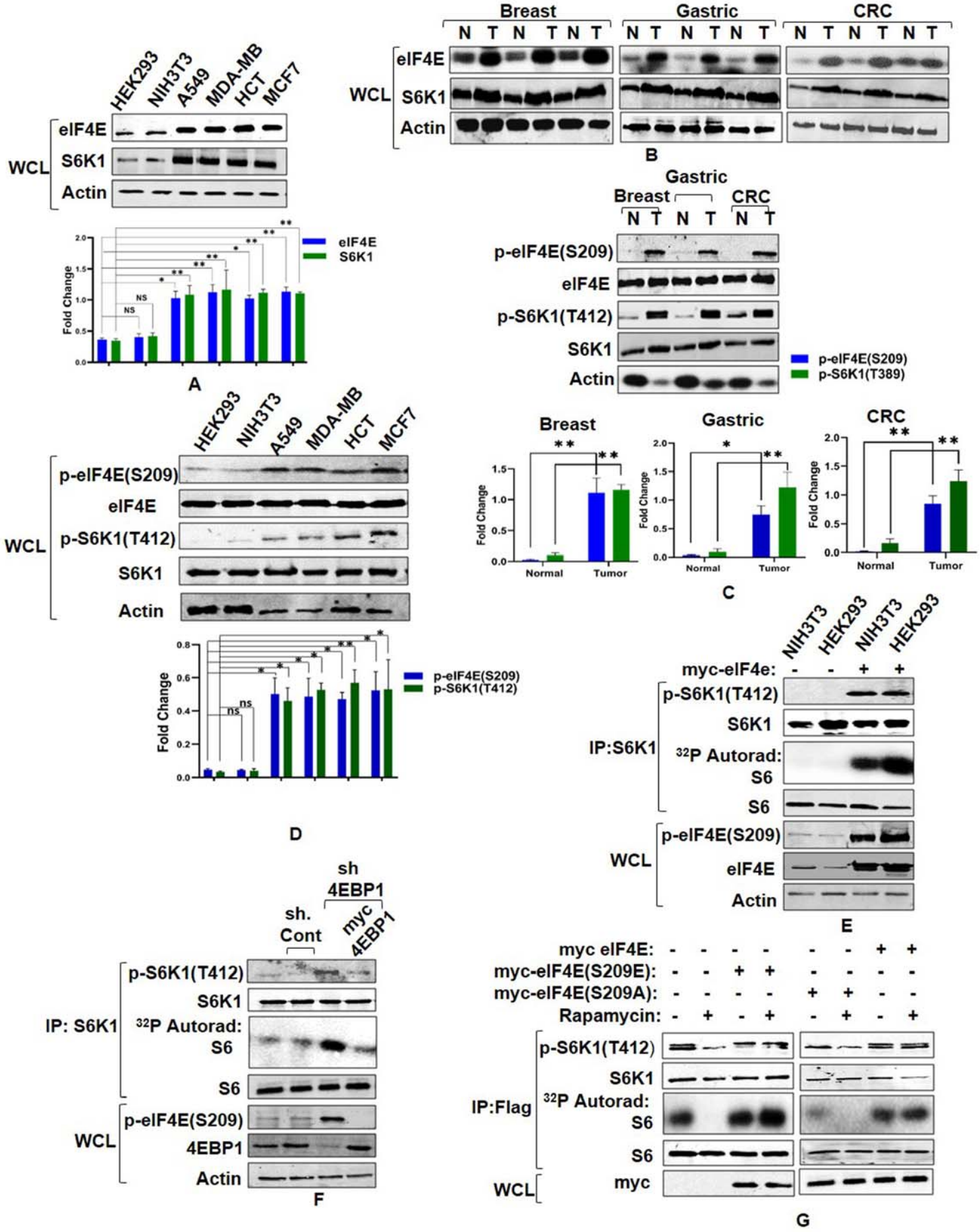
HEK293
NIH3T3
A549
MDA-MB
HCT
MCF7
WCL
eIF4E
S6K1
Actin
Fold Change
NS
A
Breast
Gastric
CRC
N T N T N T
B
p-eIF4E(S209)
p-S6K1(T412)
p-S6K1(T389)
Normal
Tumor
C
D
IP:S6K1
32P Autorad:
S6
myc-eIF4e:
NIH3T3
HEK293
E
sh. Cont
sh 4EBP1
myc 4EBP1
IP: S6K1
4EBP1
F
myc eIF4E:
myc-eIF4E(S209E):
myc-eIF4E(S209A):
Rapamycin:
IP:Flag
myc
G

Figure 1

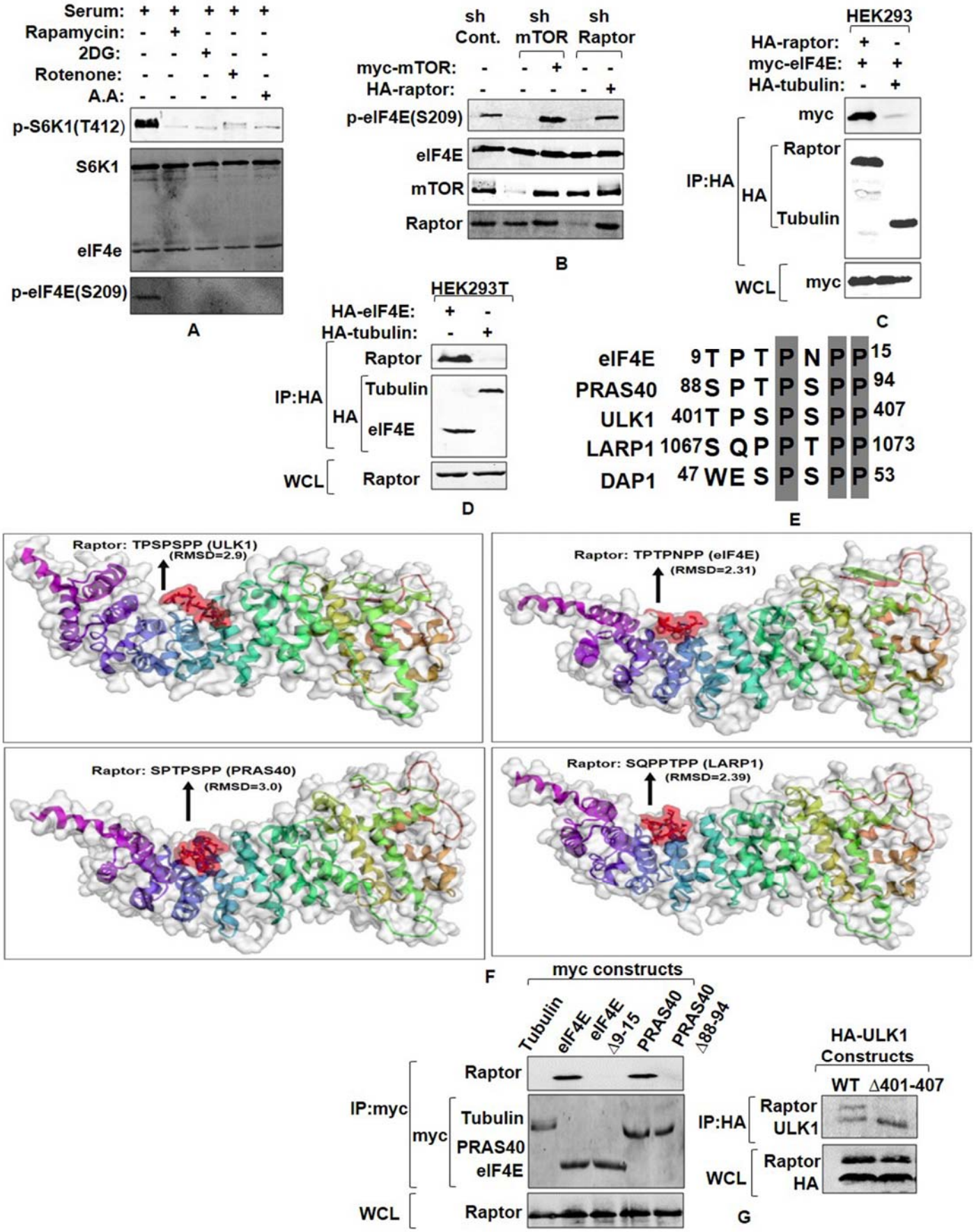
Serum: + + + + +
Rapamycin: - + - - -
2DG: - - + - -
Rotenone: - - - + -
A.A: - - - - +
p-S6K1(T412)
S6K1
eIF4e
p-eIF4E(S209)
A
sh Cont.
sh mTOR
sh Raptor
myc-mTOR: - - + - -
HA-raptor: - - - - +
p-eIF4E(S209)
eIF4E
mTOR
Raptor
B
HEK293
HA-raptor: + -
myc-eIF4E: + +
HA-tubulin: - +
myc
IP:HA
HA
Raptor
Tubulin
WCL
myc
C
HEK293T
HA-eIF4E: + -
HA-tubulin: - +
Raptor
IP:HA
HA
Tubulin
eIF4E
WCL
Raptor
D
eIF4E 9 T P T P N P P 15
PRAS40 88 S P T P S P P 94
ULK1 401 T P S P S P P 407
LARP1 1067 S Q P P T P P 1073
DAP1 47 WE S P S P P 53
E
Raptor: TPSPSPP (ULK1)
(RMSD=2.9)
Raptor: TPTPNPP (eIF4E)
(RMSD=2.31)
Raptor: SPTPSPP (PRAS40)
(RMSD=3.0)
Raptor: SQPPTPP (LARP1)
(RMSD=2.39)
F
myc constructs
Tubulin
eIF4E
eIF4E Δ9-15
PRAS40
PRAS40 Δ88-94
Raptor
IP:myc
myc
Tubulin
PRAS40
eIF4E
WCL
Raptor
HA-ULK1 Constructs
WT
Δ401-407
IP:HA
Raptor
ULK1
WCL
Raptor
HA
G

Figure 2

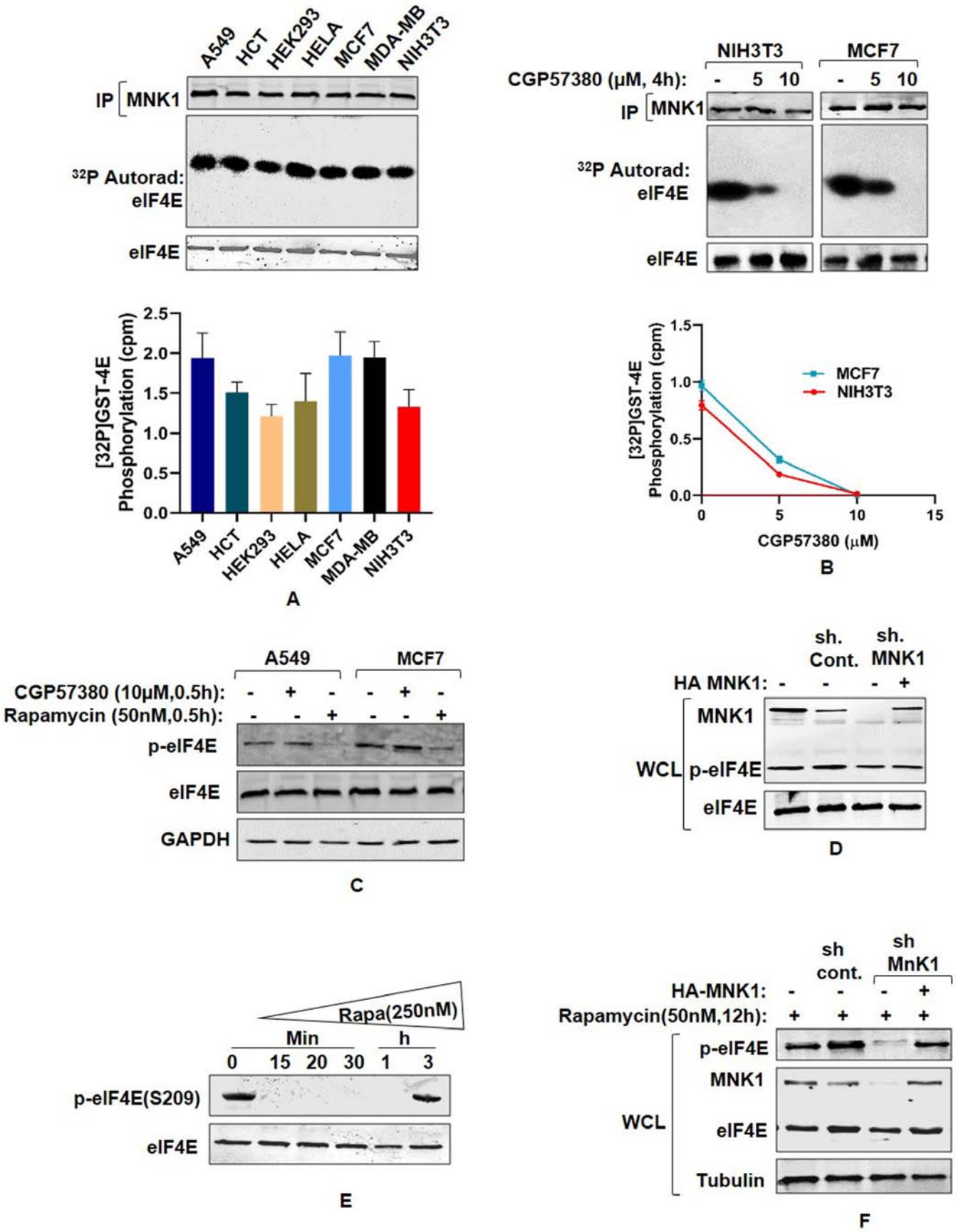
A549
HCT
HEK293
HELA
MCF7
MDA-MB
NIH3T3
IP
MNK1
32P Autorad:
eIF4E
eIF4E
[32P]GST-4E Phosphorylation (cpm)
A
NIH3T3
MCF7
CGP57380 (μM, 4h):
- 5 10
- 5 10
IP
MNK1
32P Autorad:
eIF4E
eIF4E
[32P]GST-4E Phosphorylation (cpm)
MCF7
NIH3T3
CGP57380 (μM)
B
A549
MCF7
CGP57380 (10μM,0.5h):
Rapamycin (50nM,0.5h):
p-eIF4E
eIF4E
GAPDH
C
sh. Cont.
sh. MNK1
HA MNK1:
MNK1
WCL
p-eIF4E
eIF4E
D
Rapa(250nM)
Min
h
0 15 20 30 1 3
p-eIF4E(S209)
eIF4E
E
sh cont.
sh MnK1
HA-MNK1:
Rapamycin(50nM,12h):
p-eIF4E
MNK1
WCL
eIF4E
Tubulin
F

Figure 3

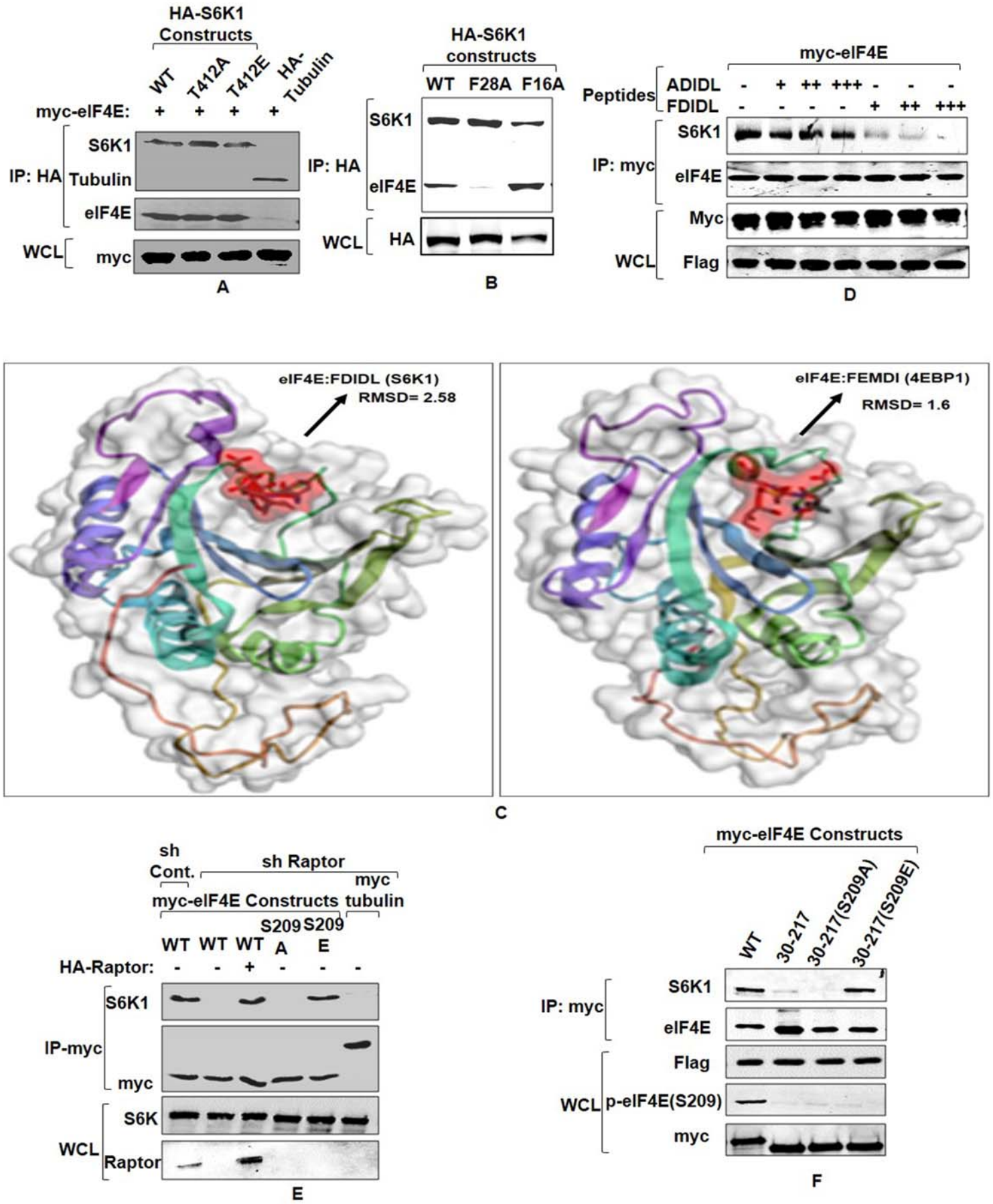
HA-S6K1 Constructs
WT
T412A
T412E
HA-Tubulin
myc-eIF4E:
IP: HA
S6K1
Tubulin
eIF4E
WCL
myc
A
HA-S6K1 constructs
WT
F28A
F16A
S6K1
eIF4E
IP: HA
WCL
HA
B
myc-eIF4E
Peptides
ADIDL
FDIDL
IP: myc
S6K1
eIF4E
Myc
WCL
Flag
D
eIF4E:FDIDL (S6K1)
RMSD= 2.58
eIF4E:FEMDI (4EBP1)
RMSD= 1.6
C
sh Cont.
sh Raptor
myc-eIF4E Constructs
myc
tubulin
S209 A
S209 E
HA-Raptor:
IP-myc
S6K1
myc
WCL
S6K
Raptor
E
myc-eIF4E Constructs
WT
30-217
30-217(S209A)
30-217(S209E)
IP: myc
S6K1
eIF4E
Flag
WCL
p-eIF4E(S209)
myc
F

Figure 4

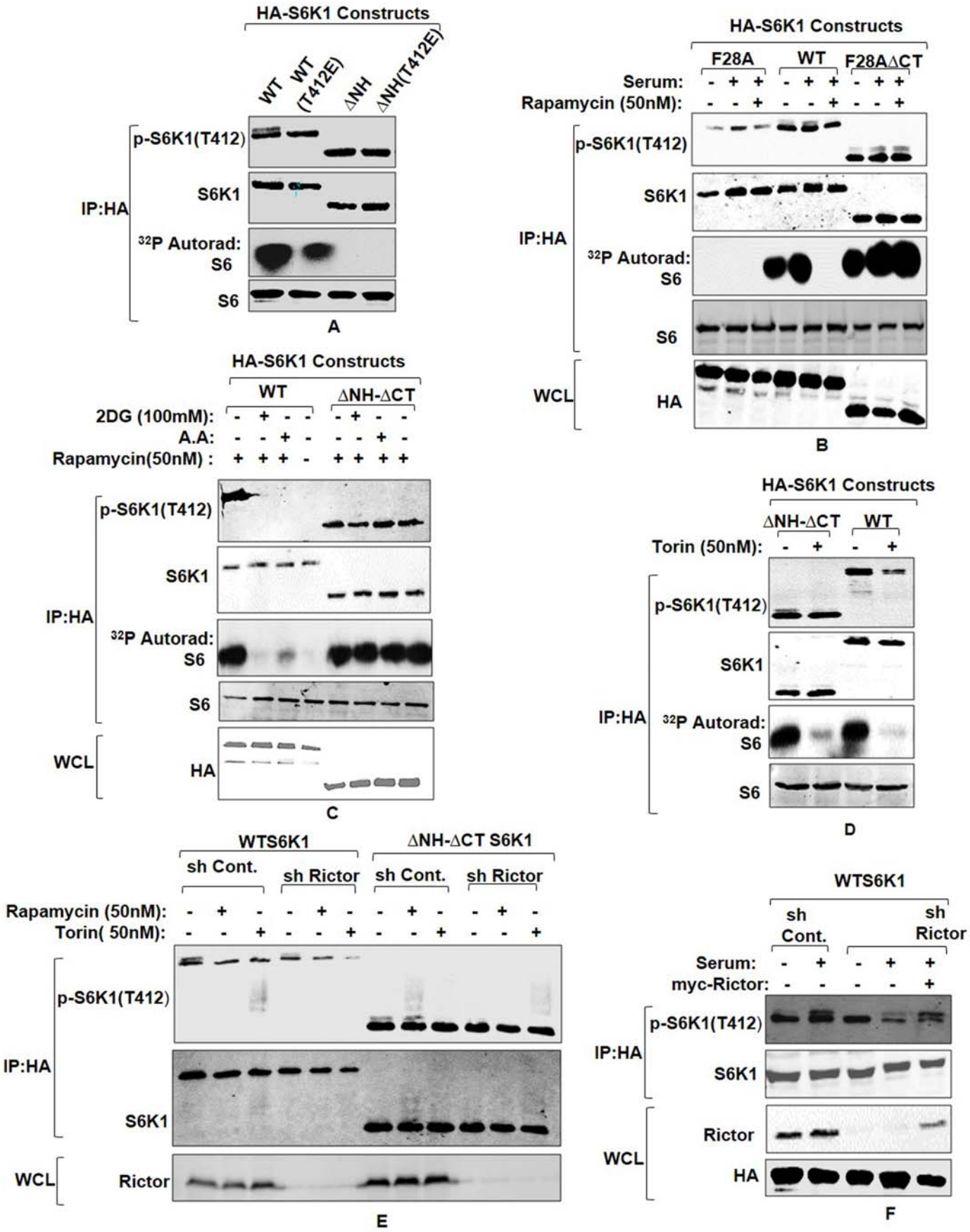
HA-S6K1 Constructs
WT
WT (T412E)
ΔNH
ΔNH(T412E)
IP:HA
p-S6K1(T412)
S6K1
32P Autorad: S6
S6
A
HA-S6K1 Constructs
F28A
WT
F28AΔCT
Serum:
Rapamycin (50nM):
IP:HA
p-S6K1(T412)
S6K1
32P Autorad: S6
S6
WCL
HA
B
HA-S6K1 Constructs
WT
ΔNH-ΔCT
2DG (100mM):
A.A:
Rapamycin(50nM) :
IP:HA
p-S6K1(T412)
S6K1
32P Autorad: S6
S6
WCL
HA
C
HA-S6K1 Constructs
ΔNH-ΔCT
WT
Torin (50nM):
IP:HA
p-S6K1(T412)
S6K1
32P Autorad: S6
S6
D
WTS6K1
ΔNH-ΔCT S6K1
sh Cont.
sh Rictor
sh Cont.
sh Rictor
Rapamycin (50nM):
Torin(50nM):
IP:HA
p-S6K1(T412)
S6K1
WCL
Rictor
E
WTS6K1
sh Cont.
sh Rictor
Serum:
myc-Rictor:
IP:HA
p-S6K1(T412)
S6K1
WCL
Rictor
HA
F

Figure 5

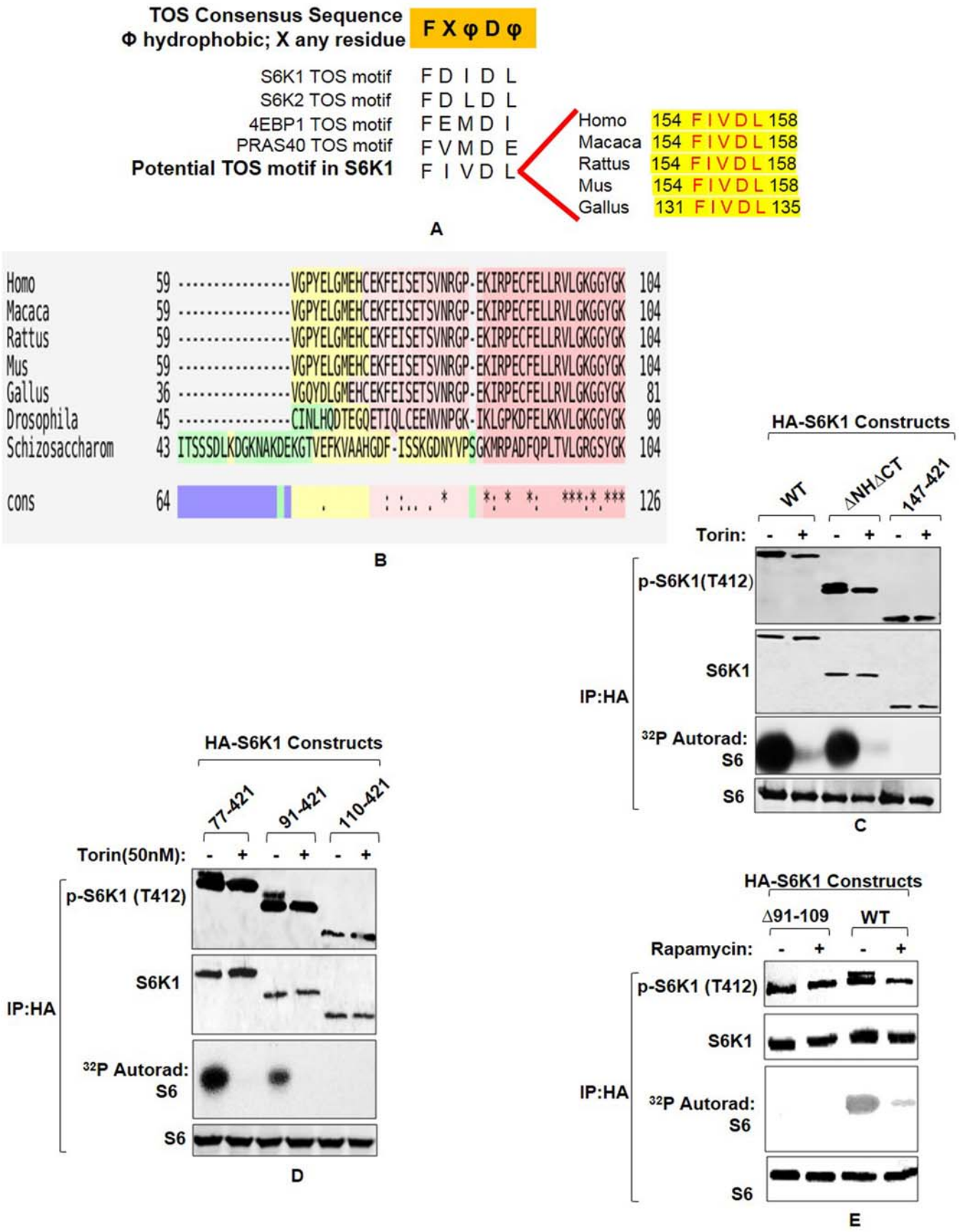
TOS Consensus Sequence
Φ hydrophobic; X any residue
F X φ D φ
S6K1 TOS motif F D I D L
S6K2 TOS motif F D L D L
4EBP1 TOS motif F E M D I
PRAS40 TOS motif F V M D E
Potential TOS motif in S6K1 F I V D L
Homo 154 F I V D L 158
Macaca 154 F I V D L 158
Rattus 154 F I V D L 158
Mus 154 F I V D L 158
Gallus 131 F I V D L 135
A
Homo 59 VGPYELGMEHCEKFEISETSVNRGP-EKIRPECFELLRVLGKGGYGK 104
Macaca 59 VGPYELGMEHCEKFEISETSVNRGP-EKIRPECFELLRVLGKGGYGK 104
Rattus 59 VGPYELGMEHCEKFEISETSVNRGP-EKIRPECFELLRVLGKGGYGK 104
Mus 59 VGPYELGMEHCEKFEISETSVNRGP-EKIRPECFELLRVLGKGGYGK 104
Gallus 36 VGQYDLGMEHCEKFEISETSVNRGP-EKIRPECFELLRVLGKGGYGK 81
Drosophila 45 CINLHQDTEGQETIQLCEENVNPGK-IKLGPKDFELKKVLGKGGYGK 90
Schizosaccharom 43 ITSSSDLKDGKNAKDEKGTVEFKVAAHGDF-ISSKGDNYVPSGKMRPADFQPLTVLGRGSYGK 104
cons 64 126
B
HA-S6K1 Constructs
WT
ΔNHΔCT
147-421
Torin: - + - + - +
p-S6K1(T412)
S6K1
IP:HA
32P Autorad: S6
S6
C
HA-S6K1 Constructs
77-421
91-421
110-421
Torin(50nM): - + - + - +
p-S6K1 (T412)
S6K1
IP:HA
32P Autorad: S6
S6
D
HA-S6K1 Constructs
Δ91-109
WT
Rapamycin: - + - +
p-S6K1 (T412)
S6K1
IP:HA
32P Autorad: S6
S6
E

Figure 6

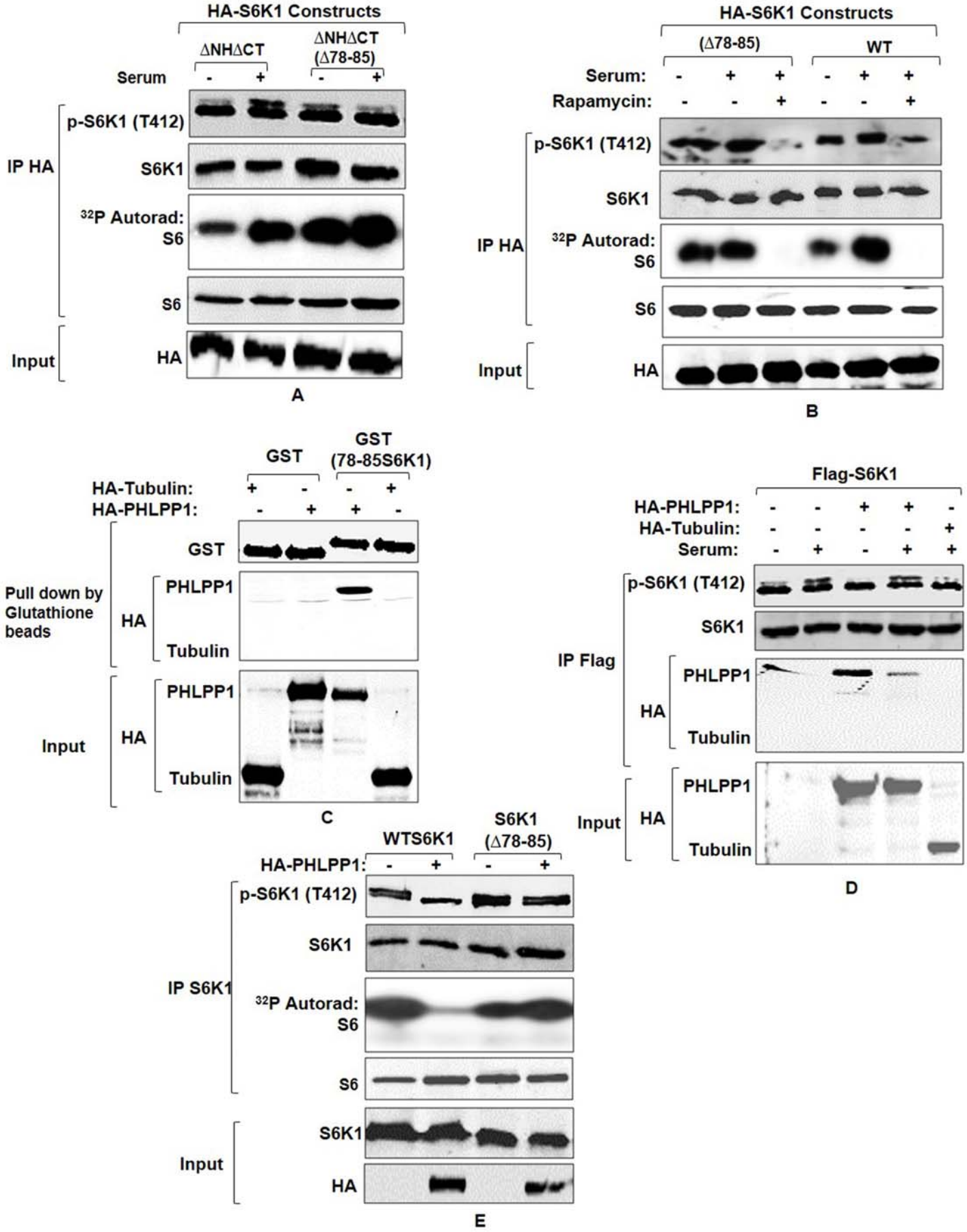
HA-S6K1 Constructs
ΔNHΔCT
ΔNHΔCT (Δ78-85)
Serum
- + - +
p-S6K1 (T412)
S6K1
IP HA
32P Autorad: S6
S6
Input
HA
A
HA-S6K1 Constructs
(Δ78-85)
WT
Serum: - + + - + +
Rapamycin: - - + - - +
p-S6K1 (T412)
S6K1
IP HA
32P Autorad: S6
S6
Input
HA
B
GST
GST (78-85S6K1)
HA-Tubulin: + - - +
HA-PHLPP1: - + + -
GST
Pull down by Glutathione beads
HA
PHLPP1
Tubulin
Input
HA
PHLPP1
Tubulin
C
Flag-S6K1
HA-PHLPP1: - - + + -
HA-Tubulin: - - - - +
Serum: - + - + +
p-S6K1 (T412)
S6K1
IP Flag
HA
PHLPP1
Tubulin
Input
HA
PHLPP1
Tubulin
D
WTS6K1
S6K1 (Δ78-85)
HA-PHLPP1: - + - +
p-S6K1 (T412)
S6K1
IP S6K1
32P Autorad: S6
S6
Input
S6K1
HA
E

Figure 7

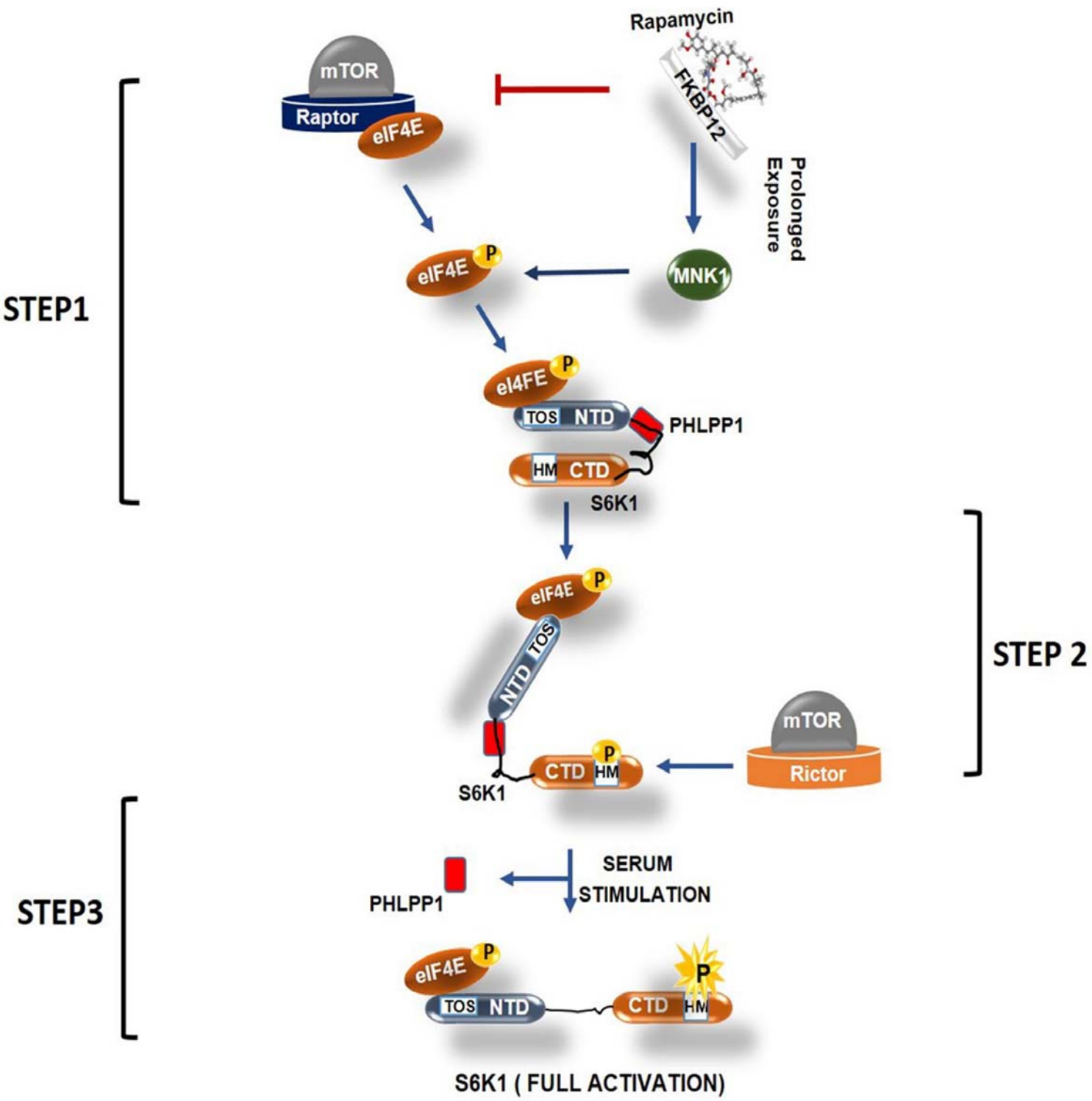
Rapamycin
mTOR
Raptor
eIF4E
FKBP12
Prolonged Exposure
eIF4E
P
MNK1
STEP1
eI4FE
P
TOS
NTD
PHLPP1
HM
CTD
S6K1
eIF4E
P
NTD
TOS
mTOR
Rictor
STEP 2
CTD
P
HM
S6K1
STEP3
PHLPP1
SERUM
STIMULATION
eIF4E
P
TOS
NTD
P
CTD
HM
S6K1 (FULL ACTIVATION)

Figure8

Supplementary Information

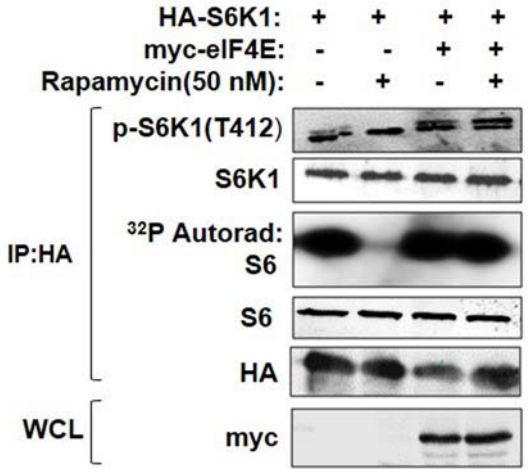

Fig S1: Overexpression of eIF4E renders S6K1 rapamycin resistant.
Plasmids encoding HA-S6K1 were either transfected alone or along with myc-eIF4E in HEK293 cells in indicated manner. 60 hours post transfection, cells were either lysed directly or after treatment with 50 nM Rapamycin for 30 minutes. The lysates obtained were HA Immunoprecipitated. S6K1 activity was monitored using GST-S6 as substrate. The immunoblots were further probed with indicated antibodies.

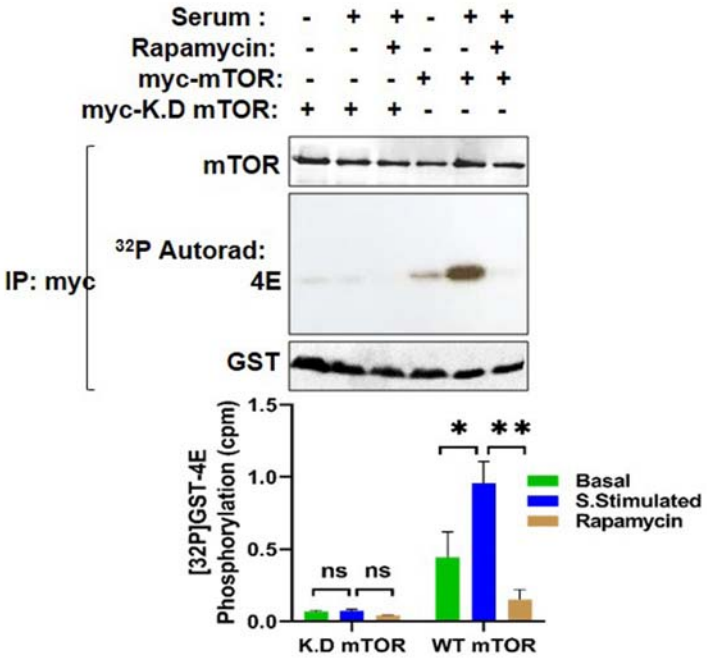

Fig S2: mTORC1 is an in vitro kinase of eIF4E.
HEK293 cells were transfected with myc tagged mTOR and its Kinase Dead variant in indicated manner. The cells were serum starved and lysed directly or after serum stimulation in presence or absence of 50 nM rapamycin for 30 min. The lysates were subjected to myc-IP and followed by kinase assay using GST-4E as a substrate. The immunoblots were further probed with indicated antibodies.

Fig S4: Effect of rapamycin on phospho eIF4E levels.

(A-B) HEK293T cell lines were treated with 50nM rapamycin for indicated time periods before lysis. The lysates were immunoblotted to check the levels of phospho-eIF4E as shown (A). Alternatively, rapamycin treated cells were incubated with MNK1 inhibitor, CGP57380, in indicated manner. The lysates were immunoblotted to check the levels of phospho eIF4E (B).

Fig 3, 5 are attached as PDB Files